AMERICAN ACADEMY OF OPHTHALMOLOGY®

Progression of Polypoidal Lesions Associated with Exudative Recurrence in Polypoidal Choroidal Vasculopathy

Qiyu Bo, MD,[1,2,*] Min Zhang, MD,[1,2,*] Jieqiong Chen, MD,[1,2,3] Huixun Jia, MD,[1,2] Mengxi Shen, MD,[6] Mengsha Sun, MD,[1,2] Mengqiao Xu, MD,[1,2] Jingyang Feng, MD,[1,2] Quan Yan, MD,[1,2] Yang Yu, BS,[1,2] Peirong Huang, MD,[1,2] Tong Li, MD,[1,2,3] Fenghua Wang, MD,[1,2,3,4,5] Philip J. Rosenfeld, MD, PhD,[6] Xiaodong Sun, MD, PhD[1,2,3,4,5]

Purpose: To investigate the characteristics of the branching vascular network (BVN) and polypoidal lesions in polypoidal choroidal vasculopathy (PCV) to determine near-term indicators that may predict exudative recurrence.

Design: Retrospective cohort study.

Participants: Patients with PCV receiving anti−vascular endothelial growth factor (VEGF) monotherapy or anti-VEGF plus photodynamic therapy were followed for at least 1 year using swept-source OCT angiography (SS-OCTA) imaging.

Methods: Patients were divided into 2 groups based on whether exudative recurrence occurred during follow-up. Multiple parameters were collected and compared between the 2 groups, such as age, gender, visual acuity, number of polypoidal lesions, lesion area at the first SS-OCTA visit, and total lesion area change from the first SS-OCTA visit to the last SS-OCTA visit. To evaluate the association between SS-OCTA imaging-based risk factors and the exudative recurrences, imaging features associated with PCV such as BVN growth and polypoidal lesion progression (enlargement, new appearance, and reappearance) at each follow-up visit were analyzed. The time intervals from the nonexudative visit with lesion progression to the corresponding exudative recurrence visit were documented to explore their association with exudative recurrences. Cox regression and logistic regression analyses were used.

Main Outcome Measures: Association between BVN growth and polypoidal lesion progression with exudative recurrence.

Results: Thirty-one eyes of 31 patients (61% men) were included. Sixteen eyes had no recurrence of exudation, and 15 eyes had recurrence during follow-up. The average follow-up duration was 20.55 ± 6.86 months (range, 12−36 months). Overall, the recurrence group had worse best-corrected visual acuity ($P = 0.019$) and a greater increase in lesion area ($P = 0.010$). Logistical regression analysis showed that polypoidal lesion progression, including new appearance, enlargement, and reappearance of polypoidal lesions, was associated with exudative recurrences within 3 months (odds ratio, 26.67, 95% confidence interval, 3.77−188.54, $P = 0.001$).

Conclusions: Growth of nonexudative BVN and progression of polypoidal lesions were found to be lesion characteristics associated with exudative recurrences, and progression of polypoidal lesions might serve as a stand-alone indicator for the near-term onset of exudation. In PCV, more frequent follow-up visits are recommended when polypoidal lesions show progression. *Ophthalmology 2023;130:167-178 © 2022 by the American Academy of Ophthalmology. This is an open access article under the CC BY-NC-ND license (http://creativecommons.org/licenses/by-nc-nd/4.0/).*

Supplemental material available at www.aaojournal.org.

Polypoidal choroidal vasculopathy (PCV) is a subtype of age-related macular degeneration and is particularly prevalent in Asia.[1] Polypoidal choroidal vasculopathy is characterized by a type 1 neovascular network with the branching vascular network (BVN) and polypoidal lesions.[2-4] These polypoidal lesions were first described by Yannuzzi et al in 1990,[5] with photodynamic therapy (PDT) being the first widely used treatment.[6] Regression of the polypoidal lesions became one of the key end points for the management of PCV.

More recently, several pivotal multicenter clinical trials, such as the LAPTOP study,[7] EVEREST II study,[8] and PLANET study,[9] suggested that polypoidal lesion regression was not always necessary for visual acuity improvement. Photodynamic therapy also carries risks of recurrent hemorrhage and late-stage atrophy.[10] Currently, intravitreal injections of vascular endothelial growth factor (VEGF) inhibitors (anti-VEGF therapy) alone or in combination with PDT are considered the standard of care.[11,12] However, with the primary goal of PCV

https://doi.org/10.1016/j.ophtha.2022.09.013
ISSN 0161-6420/22

management being to improve and maintain visual acuity by minimizing exudation rather than requiring the regression of all polypoidal lesions, clinicians tend to pay more attention to exudative changes detected on OCT, such as intraretinal fluid (IRF), subretinal fluid (SRF), and fluid or hemorrhage under the retinal pigment epithelium (RPE) layer during treatment and follow-up.[13-15]

Although eyes with PCV generally respond well to anti-VEGF treatment in the early stages of treatment,[16,17] the effects of anti-VEGF agents on the regression of BVN and polypoidal lesions are limited. Studies have shown that approximately half of patients experienced a decline in their best-corrected visual acuity (BCVA) to baseline after 3 to 5 years of follow-up due to repeated exudative recurrences.[18-20] Persistent BVN and polypoidal lesions appear to be major risk factors for exudative recurrence.[21-23] In addition, Kwon et al[24] found that the progression of PCV lesions without concurrent fluid preceded exudative recurrences, which suggests that the presence of BVN together with polypoidal lesions either predisposes to exudative recurrences or is responding to the same stimulus that leads to exudative recurrences. Although previous studies have indicated a close association between changes in BVN and polypoidal lesions with exudative recurrences in PCV over a period of years,[25,26] predictors of near-term recurrence have not been well investigated. Therefore, in this study, we aimed to explore whether progression of BVN or polypoidal lesions during follow-up could serve as harbingers of near-term exudative recurrences.

To investigate the morphological characteristics of BVN and polypoidal lesions before and at the time of exudative recurrence and to confirm whether the overall lesion progression is associated with exudation and whether there is a difference in BVN growth versus polypoidal lesion progression, we reviewed patients with PCV followed up for at least 1 year using swept-source OCT angiography (SS-OCTA) imaging. We studied the morphological characteristics of BVN and polypoidal lesions before and during anti-VEGF therapy, with or without PDT, to identify potential SS-OCTA morphological characteristics associated with PCV exudative recurrences.

Methods

This study was a retrospective, observational, consecutive case series. Patients with PCV who received anti-VEGF or PDT and were consecutively followed up for at least 1 year using SS-OCTA at the Shanghai General Hospital, Shanghai, China, from December 2017 to June 2021 were enrolled. This study was approved by the Institutional Review Board of Shanghai General Hospital and conducted in accordance with the tenets of the Declaration of Helsinki. The Institutional Review Board waived the requirement for written consent because of the retrospective nature of the study. All analyzed data were anonymized and deidentified.

Patient Selection

Patients enrolled in this study were diagnosed with PCV, which was confirmed by 2 experienced ophthalmologists (F.W. and X.S.), as described next. They were followed up for at least 1 year with comprehensive clinical examination and SS-OCTA imaging (PLEX Elite 9000, Carl Zeiss Meditec AG) at each visit. Swept-source OCTA images were obtained using the 6 × 6-mm and 3 × 3-mm scan patterns. Only 1 eye from each patient was included in this study. For patients with bilateral PCV, the eye with a treatment-naive lesion at the first examination was enrolled preferentially, and for patients with bilateral treatment-naive PCV lesions, the eye with the longer follow-up duration was chosen.

The diagnostic criteria for PCV were modified from several published studies based on multimodal imaging, including color fundus imaging (Visucam 200 Digital Fundus Camera; Carl Zeiss Meditec AG), simultaneous fluorescein angiography, indocyanine green angiography imaging (ICGA) (Spectralis; Heidelberg Engineering, Inc), structural OCT (Spectralis; Heidelberg Engineering, Inc), and SS-OCTA. Traditionally, the diagnosis of PCV was made by the presence of punctate hyperfluorescent spots on ICGA and at least 1 of the following clinical or angiographic findings: BVN, pulsatile polypoidal lesions, orange subretinal nodule, hypofluorescent halo, or association with massive submacular hemorrhage.[27] If ICGA was unavailable, 2 of the following 3 requirements had to be satisfied: (1) notched/narrow-peaked posterior pigment epithelial detachment (PED), (2) hyperreflective ring under the PED, and (3) notched or hemorrhagic PED on color fundus imaging.[28] Cases with OCT-based major criteria (sub-RPE ringlike lesion, en face OCT complex RPE elevation, and sharp-peaked PED) along with tangled or coillike structures on en face SS-OCTA were also diagnosed as PCV.[2,29,30]

The exclusion criteria included (1) a history of intraocular surgery other than cataract surgery; (2) a large detachment of the RPE or hemorrhage obscuring the BVN or polypoidal lesions; (3) severe media opacity; (4) excess motion artifacts; (5) macular neovascularization (MNV) secondary to high myopia (≥ -6.00 diopters); (6) history of other ocular diseases, such as glaucoma, diabetic retinopathy, uveitis, and endophthalmitis; (7) treatment-naive patients with a dry macula at baseline who experienced only 1 episode of exudation during the follow-up period; and (8) persistent exudation that never resolved during the follow-up period.

Treatment Strategies

For treatment-naive exudative eyes, 3 initial loading doses of intravitreal anti-VEGF therapy were administered, followed by monthly injections until a dry macula was achieved, which was considered the first remission. A dry macula was defined by the absence of any retinal fluid detected by OCT, with or without the existence of fluid under the RPE. Subsequently, a pro re nata or treat-and-extend regimen was used when exudation recurred. For previously treated exudative eyes, a pro re nata or treat-and-extend regimen was used according to the decisions of experienced ophthalmologists. With the pro re nata regimen, additional injections were administered when macular exudative changes were observed, including enlargement of serous PEDs. If IRF or SRF persisted but was stable for consecutive visits, the injections could be skipped. With the treat-and-extend regimen, follow-up visits and treatments were extended by 2-week intervals when no signs of exudative change were present. However, if any signs of exudation were detected, the treatment intervals were shortened by 2 weeks. Anti-VEGF treatment was administered at every visit regardless of any exudative changes, but the follow-up intervals were individualized. The treatment intervals ranged from a minimum of 4 weeks to a maximum of 3 months. In addition, only a few patients with poor responses to anti-VEGF therapy were treated with PDT during the follow-up period before 2019, when the verteporfin was still commercially available.

Grouping and Definition of Exudative Recurrence

To analyze the risk factors related to exudative recurrence, patients were first divided into 2 groups based on whether the exudative recurrence occurred during the SS-OCTA follow-up visits.

Exudative recurrence in this study was defined as the reappearance of IRF, SRF, or serous PED on OCT, or new subretinal or sub-RPE hemorrhages, after the previous visit showed a fluid-free (dry) macula. Enlargement of any persistent exudation (SRF/IRF/serous PED) was not considered as exudative recurrence.

For previously treated eyes with a dry macula at baseline, which corresponded to the earliest SS-OCTA visit, recurrence of exudation was considered as the first appearance of exudative features or the reappearance of exudative features since the last previous visit with a dry macula in the case of multiple recurrences.

For treatment-naive eyes with a dry macula at baseline, which corresponded to the earliest SS-OCTA visit, recurrence of exudation was considered as the second or subsequent reappearance of exudation, whereas the first episode of exudation was not counted as an exudative recurrence.

For both previously treated and treatment-naive eyes with exudation at their earliest SS-OCTA visit, exudative recurrence was assessed from the first time a dry macula was observed after treatment during follow-up visits. If the patients had persistent exudation since their first SS-OCTA visit and the fluid never resolved during follow-up visits, then the patients would not be enrolled in the study.

Risk Factor Analyses for Exudative Recurrence

To analyze the risk factors for recurrence of exudation, demographic data (age and gender), medical history, and lesion characteristics were collected, reviewed, and compared, including logarithm of the minimum angle of resolution (logMAR) BCVA, subfoveal choroid thickness (SFCT), number of intravitreal injections, follow-up duration, lesion area at baseline (first SS-OCTA visit), total lesion area change calculated by comparing the lesion areas at the first and the last SS-OCTA visits, and the number of polypoidal lesions. The SFCT was measured as the subfoveal distance from the Bruch membrane to the sclerochoroidal interface on the structural OCT images using the instrument's calipers.

The RPE-RPE fit segmentation was used to visualize the BVN and polypoidal lesions. The 2 segmentation lines were manually adjusted when necessary to optimally visualize the lesions, and the segmentation remained consistent during the follow-up visits. Artifacts in OCTA images of the outer retina were removed by using the automated projection artifact removal software integrated into the instrument.

Exudative Recurrences and Characteristics of Lesion Progression on SS-OCTA

Morphological progression patterns of BVN and polypoidal lesions showed on SS-OCTA were compared between patients with and without exudative recurrences. Swept-source OCTA images at each visit were collected and reviewed by 2 experienced attending physicians (Q.B. and T.L.) independently. Any disagreement was resolved by open arbitration between 2 retina specialists (X.S. and F.W.). Morphological changes of BVN and polypoidal lesion on SS-OCTA (Fig 1) were defined in accordance with standards based on ICGA imaging:[31] (1) growth: $\geq$ 10% increase in BVN area compared with the previous examination; (2) shrinkage: $\geq$ 10% decrease in BVN area compared with the previous examination; (3) progression: $\geq$ 10% hyperreflective area enlargement, new appearance, or reappearance of polypoidal lesions compared with previous examination; (4) reduction: a decrease in the number of or $\geq$ 10% decrease in the area of polypoidal lesions compared with the previous examination; (5) complete regression: no polypoidal lesions observed on images; (6) no change: $<$ 10% change in BVN or polypoidal lesion area compared with the previous examination.

Measurements of Intervals from Lesion Progression to Exudative Recurrence

To evaluate the association between lesion progression and exudative recurrence, we assessed whether the interval for BVN growth or polypoidal lesion progression to the corresponding exudation visit was associated with the recurrence of exudation. The time interval between the most recent nonexudative visit with evidence of lesion progression and the corresponding recurrence visit was measured. Flow charts (Fig S2, available at www.aaojournal.org) were created to show the stepwise decision process of defining and measuring time intervals for lesion progression to exudative recurrence, with a modified figure showing examples of quantification (Fig S3, available at www.aaojournal.org). Briefly, after identification of the recurrence visit, the most recent nonexudative visit with evidence of progressive changes was then determined by comparing the OCTA-morphological features with those of the corresponding recurrence visit. For eyes experiencing multiple recurrences during the follow-up period, the mean time interval from each lesion progression to the corresponding exudative recurrence was calculated for subsequent statistical analyses.

Quantitation of Polypoidal Lesion and BVN on SS-OCTA Imaging

Quantification of the lesion area was based on both SS-OCTA en face and B-scans for both the flow and structural images. The 6 $\times$ 6-mm SS-OCT scan patterns were applied to assess the lesion characteristics based on the overall lesion size. Polypoidal lesions and BVN were identified as previously described.[31] The sizes of the polypoidal lesions or BVN on SS-OCTA imaging were measured by exporting the en face RPE-RPE fit images in a TIFF format. The regions of polypoidal lesions or BVN were then manually outlined by 2 graders (Q.B. and T.L.) according to the hyperreflective area on en face images, the contour of which corresponded to the boundaries of the neovascular PED, or double-layer sign detected on cross-sectional B-scans. The outlined region was measured using Photoshop CS6 (version 13.0.0.0, Adobe). In cases where lesion boundaries were ambiguous, both graders reached an agreement on the lesion area before drawing the final outlines separately. ImageJ software (version 1.8.0_172 64-bit for Mac, National Institutes of Health) was used to measure the outlined lesion areas by 2 other graders independently (M.S. and M.X., masked to participant information). Figure S3 was created to show an example of lesion measurements.

Statistical Analyses

For patients with multiple episodes of exudation, mean values were used for statistical analyses. The normality of the continuous parameters was tested with the Shapiro–Wilk test. The main outcomes are presented as mean $\pm$ standard deviations or medians with ranges. The independent sample Student t test (P values adjusted when equal variable not obtained) and Wilcoxon Mann–Whitney test were applied, as appropriate, to evaluate the variables of factors between 2 groups. The paired-samples t test and related-samples Wilcoxon signed-rank test were used to test the differences of parameters recorded in both the first and the last visits, such as logMAR BCVA, SFCT, and lesion area. Categorical variables, such as the distribution

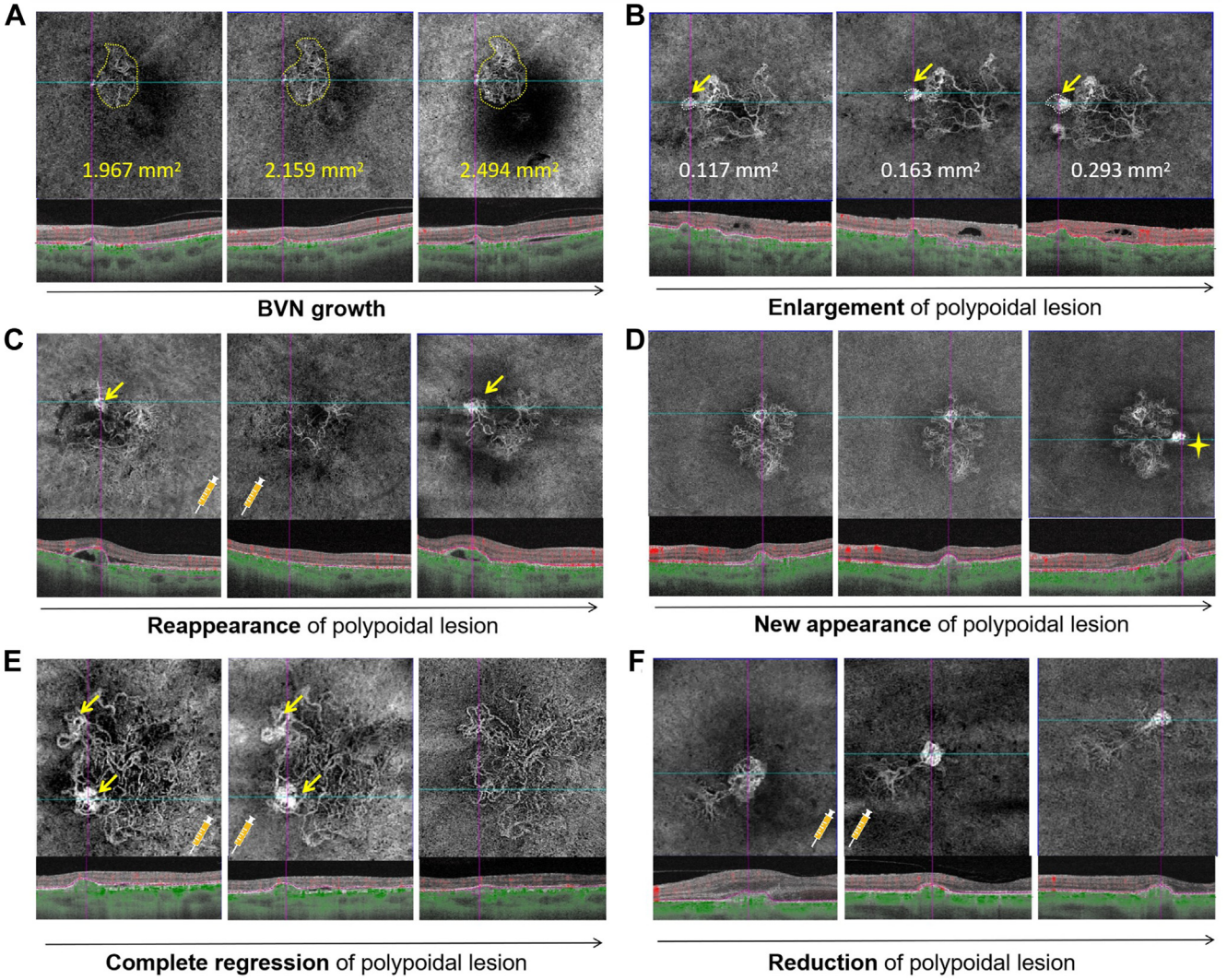

Figure 1. Examples of swept-source OCT angiography (SS-OCTA) imaging features showing branching vascular network (BVN) growth, polypoidal lesion progression (enlargement, reappearance, and new appearance of polypoidal lesions), complete regression, and reduction of polypoidal lesions. **A,** En face SS-OCTA images showing increased BVN area (yellow circles) in 3 follow-up visits without treatment. **B,** En face SS-OCTA images showing area enlargement of polypoidal lesions (white circle) in 3 follow-up visits without treatment. **C,** En face SS-OCTA images showing regression of a polypoidal lesion after anti-vascular endothelial growth factor (VEGF) treatment; however, the polypoidal lesion reappeared (yellow arrow) at a subsequent visit. **D,** En face SS-OCTA images showing the new appearance of 1 polypoidal lesion (yellow asterisk) in the third follow-up visit without treatment. **E,** En face SS-OCTA images showing complete regression of polypoidal lesions (yellow arrows) after anti-VEGF treatment with the stable appearance of type 1 macular neovascularization. **F,** En face SS-OCTA images showing reduction in the size of a polypoidal lesion after anti-VEGF treatment.

of morphological changes among different subgroups, were tested with the chi-square test or Fisher exact test. The Kaplan–Meier test (log-rank) was used to evaluate the median number of months elapsed before exudative recurrence. Hazard ratio and odds ratio (OR) were calculated by Cox regression and logistic regression and were used to evaluate the short-term (3-month interval) association potentials. Statistical analyses were performed using SPSS (version 26 for Mac, IBM). Results with P values < 0.05 were considered statistically significant.

Results

A total of 40 eyes met the inclusion criteria initially, but 6 eyes were excluded because of poor SS-OCTA image quality, and 3 eyes were excluded because of persistent exudation. A total of 31 eyes from 31 patients (61% male) were included in this study, with a mean age of 68.16 ± 5.61 years. Among them, 15 eyes were followed up because they were treatment-naive, 13 had received multiple anti-VEGF treatments, and 3 underwent multiple combinations of anti-VEGF treatments and PDT before the first SS-OCTA visit. The median follow-up duration was 20.55 ± 6.86 (range, 12–36) months. The median logMAR BCVA was 0.40 (range, 0.00–1.31) at the first visit and 0.30 (range, 0.00–2.01) at the last visit ($P = 0.625$, reported by related-samples Wilcoxon signed-rank test). There were 59 polypoidal lesions in total at the first visit and 43 at the last visit (fading rate: 27.12%), whereas only 16.13% (5/31) of eyes had complete polypoidal lesion regression at the last visit. The median total lesion area was 1.85 mm^2 (range, 0.29–6.75) at the first visit and 2.30 mm^2 (range, 0.29–7.38) at the

last visit ($P = 0.013$, reported by related-samples Wilcoxon signed-rank test), and the total lesion area was enlarged by $+0.42 \pm 0.83$ mm^2, suggesting the existence of lesion progression in eyes with PCV during treatments and follow-up.

Patients with PCV were divided into 2 groups based on exudative recurrence during the follow-up visits: the recurrence group (n = 15) and the no recurrence group (n = 16). Of note, 3 patients experienced multiple recurrences of exudation, and the other 12 patients experienced recurrence only once. Demographic and clinical characteristics of the 2 groups are summarized in Table 1, with detailed information for each patient shown in Table S2 (available at www.aaojournal.org). There were no differences between the 2 groups in terms of age, gender, follow-up duration, logMAR BCVA at the first visit, number of anti-VEGF treatments before and during follow-up visits, lesion area at the first visit, and SFCT at the first and last visits ($P > 0.05$).

The recurrence group had poorer BCVA at the last visit (recurrence vs. no recurrence, median logMAR BCVA 0.22 vs. 0.52; $P = 0.019$), indicating worse visual prognosis in the recurrence group than in the no recurrence group. In addition, the recurrence group had a total lesion area growth of 0.82 ± 0.99 mm^2 during follow-up visits, which is larger than that in the no recurrence group (0.03 ± 0.36 mm^2; $P = 0.010$). The variability in the follow-up periods was adjusted so that the total lesion area change per year was evaluated. The recurrence group showed a more rapid change per year of total lesion area enlargement than the no recurrence group (0.44 ± 0.61 mm^2/year vs. 0.00 ± 0.25 mm^2/year, $P = 0.007$; related-samples Wilcoxon signed-rank test). These results highlight that lesion progression was a risk factor for exudative recurrence and poor visual prognosis. Although not statistically significant, the mean SFCT at the first visit in the no recurrence group was smaller than that in the recurrence group (258.50 ± 70.27 μm vs. 289.40 ± 86.03 μm; $P = 0.281$).

Exudative Recurrence-Related Morphological Characteristics Included BVN Growth and Polypoidal Lesion Progression

Exudation-related morphological characteristics of the 31 eyes included in this study were analyzed and summarized in Table 3. Morphological characteristics of both BVN and polypoidal lesions showed different distribution patterns between patients with and without exudative recurrences. Growth of BVN was found in 13 (81.25%) eyes, and polypoidal lesion progression was found in 12 (80.00%) eyes in the recurrence group, which was greater than that in the no recurrence group (2 with BVN growth [12.50%] and 1 with polypoidal lesion progression [6.25%]). Specifically, there were 6 (50%), 9 (75%), and 6 (50%) eyes with growth, new appearance, or reappearance of polypoidal lesions, respectively, and these findings were not mutually exclusive. The recurrence group had a higher incidence of BVN growth and polypoidal lesion progression than the no recurrence group (both $P < 0.001$).

Median Time between BVN or Polypoidal Lesion Progression and the Recurrence of Exudation

Among the 15 eyes in the recurrence group, most eyes (11/15, 73.33%) had both BVN growth and polypoidal lesion progression (Fig 4A). There were 17 eyes with lesion progression, including 14 eyes from the recurrence group and 3 eyes from the no recurrence group (2 eyes with BVN growth only and 1 eye with polypoidal lesion growth only). With exudative recurrence as the end point, the risk of exudative recurrence in patients with polypoidal lesion progression was 2.84 times the risk of exudative recurrence in patients with BVN growth (95% confidence interval [CI], 1.1−6.90, $P = 0.017$), indicating a higher risk of exudative recurrence in patients with polypoidal lesion progression. In addition, the median time interval between BVN growth and recurrence was longer than that between polypoidal lesion progression and recurrence (7 months vs. 3 months, $P = 0.009$, Fig 4B and Table 4), indicating the short-term association potential of polypoidal lesion progression with exudative recurrence.

To further test this, we evaluated all recruited eyes together and used a 3-month interval as the cutoff point. Logistical regression analysis showed that only eyes with polypoidal lesion progression had an increased risk of exudative recurrence within 3 months (OR, 26.67, 95% CI, 3.77−188.54, $P = 0.001$; Table 5). Compared with BVN growth (OR, 0.573, 95% CI, 0.08−4.01, $P = 0.573$), polypoidal lesion progression was more closely associated with exudative recurrence within 3 months.

Polypoidal Lesion Progression as an Indicator of Near-Term Exudative Recurrence

Using SS-OCTA, we were able to observe the morphological changes of BVN and polypoidal lesions before and after anti-VEGF therapy. In the no recurrence group, anti-VEGF treatment effectively resolved the exudation, whereas the polypoidal lesions regressed completely after treatment and grew into type 1 MNV (Fig 1E). However, BVN and polypoidal lesions existed for 12 to 24 months or even longer when the lesion size remained stable or changed slightly (Fig 1F).

In the recurrence group, lesions were prone to relapse and recur, which coincided with the progression of BVN and polypoidal lesions (Figs 5 and 6). Nonexudative BVN growth (Fig 5) or polypoidal lesion progression (enlargement, new appearance, or reappearance; Fig 6) was found to precede exudative recurrence. Figure 7 shows a case of both nonexudative BVN growth and polypoidal lesion reappearance. The patient had asymptomatic exudation when a glomeruluslike polypoidal lesion was detected after 21 months of follow-up as a nonexudative type 1 neovascular lesion, suggesting that polypoidal lesions progressed before exudative recurrence. Figure 8 shows a similar evolutionary process before the first occurrence of exudation in 1 treatment-naive case. The BVN grew initially, whereas polypoidal lesions subsequently progressed, followed by presence of exudation. This observation indicates that polypoidal lesions may be the new-onset feature of the vascular network in PCV, and its progression appears to be the most notable anatomic finding that precedes exudation.

Discussion

In this study, we found that nonexudative BVN growth and polypoidal lesion progression were detected before the exudative recurrence of PCV, and both were biomarkers of PCV lesion activity on SS-OCTA. More importantly, the progression of polypoidal lesions, including enlargement, new appearance, or reappearance of these lesions, was strongly associated with exudative recurrence (log-rank median: 3 months, 95% CI, 2.50−3.50 months). Growth of BVN was not significant for near-term recurrence because the median interval between BVN growth and the onset of exudative recurrence was 7 months (95% CI, 4.10−9.90 months). These results suggest that polypoidal lesions are not only indicators for diagnosis and end points but also potential biomarkers that can guide follow-up and retreatment, especially if proactive therapy is performed.

Table 1. Demographics and Medical Histories of Enrolled Patients

	No Recurrence (n = 16)	Recurrence (n = 15)	P
Age, mean (SD), yrs	69.00 (5.45)	67.27 (5.82)	0.399
Gender, M/F	9/7	10/5	0.716
Follow-up duration (mos), mean (SD)	18.69 (6.11)	22.53 (7.27)	0.121
Treatment-naive, Y/N	8/8	7/8	1.000
Previous PDT, Y/N	1/15	2/13	0.600
Previous IVI counts, median (range)	1 (0–19)	0 (0 to 18)	0.953†
IVI counts during follow-ups, median (range)	3 (0–12)	6 (0 to 14)	0.151†
Treatment regimen, PRN/T&E	14/2	13/2	1.000
Choroidal thickness (μm) at first visit, mean (SD)	258.50 (70.27)	289.40 (86.03)	0.281
Choroidal thickness (μm) at last visit, mean (SD)	250.94 (67.39)	280.67 (95.14)	0.321
logMAR BCVA at first visit, median (range)	0.46 (0.00–1.31)	0.30 (0.00–1.31)	0.740†
logMAR BCVA at last visit, median (range)	0.22 (0.00–1.00)	0.52 (0.04–2.01)	**0.019***,†
Multiple polypoidal lesions at first visit (n > 2), Y/N	6/10	3/12	0.433
Lesion area (mm^2) at first visit, median (range)	1.39 (0.32–6.75)	2.27 (0.29–5.36)	0.423†
Lesion area (mm^2) at last visit, median (range)	1.50 (0.29–7.38)	2.61 (0.89–7.15)	0.093†
Total lesion area change from first to last visit (mm^2), mean (SD)	0.03 (0.36)	0.82 (0.99)	**0.010***
Total lesion area change per year (mm^2/yr), mean (SD)	0.00 (0.25)	0.44 (0.61)	**0.007***,†

Bold values indicate statistical significance. BCVA = best-corrected visual acuity; F = female; IVI = intravitreal injection; logMAR = logarithm of the minimum angle of resolution; M = male; N = No; PDT = photodynamic therapy; PRN = pro re nata; SD = standard deviation; T&E = treat-and-extend; Y = Yes.
*Indicates statistical significance.
†Wilcoxon Mann–Whitney test; otherwise, the Student *t* test was used.

Many studies have previously attempted to identify predictive factors for PCV prognosis, such as BCVA, lesion area, and number of polypoidal lesions at baseline. Our study focused on exudative recurrences and identified the risk factors for poor prognosis. We found that the recurrence and no recurrence groups in our study followed 2 patterns of PCV prognosis. In the recurrence group, PCV lesions had a relapsing and recurring evolution pattern, with larger total lesion area changes and poorer visual outcomes under the standard anti-VEGF treatment. In the no recurrence group, lesions tended to have a relatively stable course with a positive prognosis after a few anti-VEGF treatments for a mean follow-up of 18 months. Choi et al[32] also reported that 23.15% of PCV cases experienced no recurrence for over 18 months after anti-VEGF monotherapy. These 2 patterns were similar to those reported in the natural history studies,[33,34] indicating different lesion activities in PCV. These findings should alert clinicians to develop different follow-up treatment strategies for PCV lesions with different lesion activities and to pay more attention to patients with frequent lesion progression.

Several characteristics account for the lesion activity or recurrence of PCV. Branching vascular network persistence and growth were reported in approximately half of the eyes despite repeated anti-VEGF injections,[24,35] and the growth of PCV lesions after PDT was shown to have a close association with PCV recurrence.[22] In this study, we noticed that the total lesion area increased in the recurrence group, and it was more than that in the no recurrence group (0.82 ± 0.99 vs. 0.03 ± 0.36 mm^2, $P = 0.010$). In addition, we found that nonexudative BVN growth preceded recurrence in 81.25% (13/15) of eyes with exudative recurrence but in only 12.50% (2/16) of eyes with exudative resolution ($P < 0.001$, Table 3), verifying that BVN growth might be a risk factor associated with exudative recurrence. However, our analyses suggested that BVN growth might have a limited predictive value, as the interval from BVN growth onset

Table 3. Different Morphological Distribution Patterns of BVN and Polypoidal Lesions between Patients with and without Exudative Recurrences

Morphologic Changes on SS-OCTA, n (%)		No Recurrence (n = 16)	Recurrence (n = 15)	P Value
BVN area	Growth	2 (12.50)	13 (81.25)	<0.001*
	Shrinkage	4 (25.00)	0	
	No change	10 (62.50)	2 (18.75)	
Polypoidal lesions	Progression	1 (6.25)	12 (80.00)	**<0.001***
	Reduction	4 (31.25)	0	
	Complete regression	4 (13.00)	1 (6.67)	
	No change	7 (50.00)	2 (13.33)	

BVN = branch vascular network; SS-OCTA = swept-source OCT angiography.
*Indicates statistical significance. Polypoidal lesion progression included enlargement, new appearance, or reappearance of polypoidal lesions (not mutually exclusive).

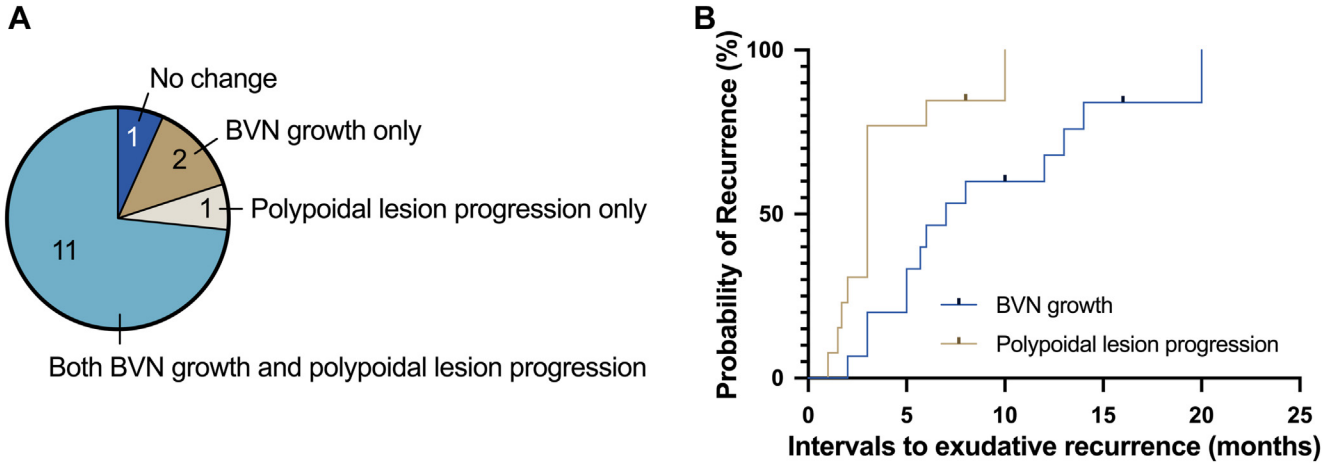

Figure 4. Distribution of lesion progression in the recurrence group and probability of recurrence based of morphological characteristics. **A,** Distribution of lesion progression in the recurrence group (n = 15), of which 73.33% were identified with both branching vascular network (BVN) growth and polypoidal lesion progression. **B,** Probability of recurrence associated with interval to recurrence (as estimated from the Cox regression model) according to the presence of BVN growth or polypoidal lesion progression.

to exudative recurrence varied from 2 to 20 months with a median recurrence time of 7 months (95% CI, 4.10−9.90) (Table 4). This is consistent with a recent report that the growth of type 1 nonexudative MNV was not correlated with near-term exudation.[36] Therefore, nonexudative BNV growth may be a recurrence-related factor but probably not a reliable predictor of near-term PCV exudative recurrence.

Polypoidal lesion progression is another hallmark of lesion activity. Remaining polypoidal lesions were once considered to be correlated with exudative recurrence.[37] However, in this study, we detected stable lesions with persistent polypoidal lesions, as well as lesions with recurrent exudation with completely regressed polypoidal lesions. Likewise, the 24-month PLANET study[9] showed that it was the active polypoidal lesions, not the burden of remaining polypoidal lesions, that influenced the overall visual outcomes. Both the PLANET study and our observations indicate that polypoidal lesions could be active or inactive. The activity, rather than the existence of polypoidal lesions, contributed to exudative recurrence.

In the present study, we found that active polypoidal lesions were not limited to lesions with exudation, and those polypoidal lesions with nonexudative progression should also be considered a risk factor. We found that polypoidal lesion progression, including the enlargement, new appearance, and reappearance, was associated with 80.00% (12/15) of cases of exudative recurrence. Most important, exudation recurred when the polypoidal lesion progression was observed in some cases (Figs 7 and 8). The time that elapsed between polypoidal lesion progression and exudation ranged from 1 to 10 months, and the median recurrence time was 3 months (95% CI, 2.70−3.30), which was shorter than that observed in BVN growth (7 months, 95% CI, 4.48−9.53 months, $P = 0.009$; Table 4). In addition, the OR for exudation after polypoidal lesion progression was 26.67 (95% CI, 3.77−188.54, $P = 0.001$; Table 5), confirming that polypoidal lesion progression was strongly associated with the near-term recurrence of exudation. Therefore, it is important to emphasize that progression of polypoidal lesions is of concern and may serve as a promising indicator for near-term recurrence and possible retreatment. More importantly, it may also suggest the possibility of a proactive re-treatment regimen when managing PCV because earlier resolution of exudation might indicate better visual prognosis.[38]

One question that needs to be addressed is whether the polypoidal lesion progression, compared with BVN growth, is an earlier and more sensitive predictor of exudative

Table 4. Intervals from Lesion Progression to the Recurrence of Exudation

	Kaplan−Meier Test (Log-Rank)		Cox Regression	
	Median Time to Recurrence of Exudation (mos, 95% CI)	P	*HR (95% CI)*	P
BVN growth	7 (4.10−9.90)	**0.009***	1.00 (reference)	**0.017***
Polypoidal lesion progression	3 (2.50−3.50)		2.84 (1.17−6.90)	

BVN = branch vascular network; CI = confidence interval; HR = hazard ratio; SE = standard error.
*Indicates statistical significance.

Table 5. Association between Lesion Progression and Recurrence

		Recurrence within 3 Mos			
		No	*Yes*	**P**	**OR (95% CI)**
BVN growth	No	14	2	0.573	0.57 (0.08–4.01)
	Yes	12	3		
Polypoidal lesion progression	No	16	2	**0.001***	26.67 (3.77–188.54)
	Yes	3	10		

BVN = branch vascular network; CI = confidence interval; OR = odds ratio.
P values were reported by logistic regression. Bold values indicate statistical significance.
*Indicates statistical significance.

recurrence. We found that, in some cases, BVN growth occurred first, followed by the progression of polypoidal lesions. As shown in Figures 7 and 8, BVN grew gradually, polypoidal lesions then progressed into glomerularlike tangles, and exudation finally occurred. These 2 cases further showed that, regardless of the natural course or pathological evolution, polypoidal lesions could be considered to represent new neovascular buds at the margins of a BVN, which further confirmed the tangled-vessel nature of polypoidal lesions, as described in our previous publication.[27,30] In addition, it has been reported that polypoidal lesions could evolve into a more typical appearance of type 1 MNV after anti-VEGF treatment,[39] suggesting that polypoidal lesions may be more responsive to anti-VEGF treatment than BVN. Polypoidal lesions with progression appeared to have more active neovascular components, which may be more prone to leakage, more responsive to treatment, and easier to regress during follow-up. This is another benefit of using polypoidal lesion progression as a potential predictor of exudation and an indicator for retreatment. Therefore, it is reasonable to consider the progression of polypoidal lesions as a new active stage of PCV that represents a budding neovascular complex arising from BVN and an important potential indicator of near-term exudative recurrence. After detection of polypoidal lesion progression on SS-OCTA, follow-up intervals should be shortened, and the possibility of proactive treatment should be considered.

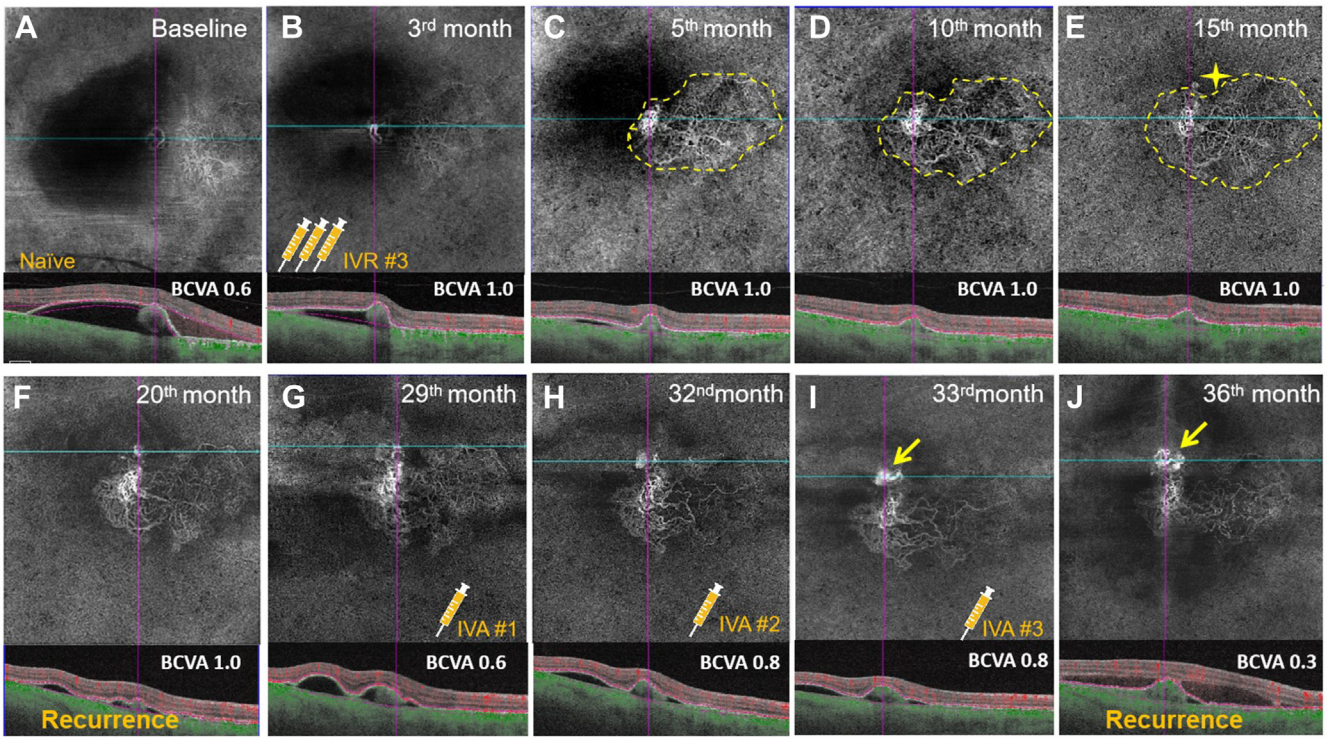

Figure 5. Swept-source OCT angiography (SS-OCTA) images showing morphological change of the branching vascular network (BVN) and polypoidal lesions in a treatment-naive eye with polypoidal choroidal vasculopathy (PCV). **A,** The 6 × 6-mm en face SS-OCTA and corresponding OCT B-scan images show an exudative PCV lesion at baseline. **B,** Regression of polypoidal lesion, subretinal fluid (SRF), and retinal pigment epithelial detachment (PED) after 3 monthly intravitreal injections of ranibizumab (IVR). **C–E,** However, nonexudative BVN growth (yellow circles) and a subsequent new appearance of a polypoidal lesion (yellow asterisk) is observed from the 5-month visit to the 15-month visit. **F.** At the 20-month visit, the first exudative recurrence is detected with reoccurrence of PED. **G,** Enlargement of the newborn polypoidal lesion and more serious PED are observed at the 29-month visit without treatment for 9 months because of the coronavirus disease 2019 pandemic, and the first intravitreal injection of aflibercept (IVA) was administered at this visit. **H, I,** Exudation has resolved after the second and third injections after the 29-month visit. **J,** However, the second exudative recurrence occurred at the 36-month visit showing with SRF. Enlargement of the polypoidal lesion was observed when compared with the previous 33-month visit. BCVA = best-corrected visual acuity.

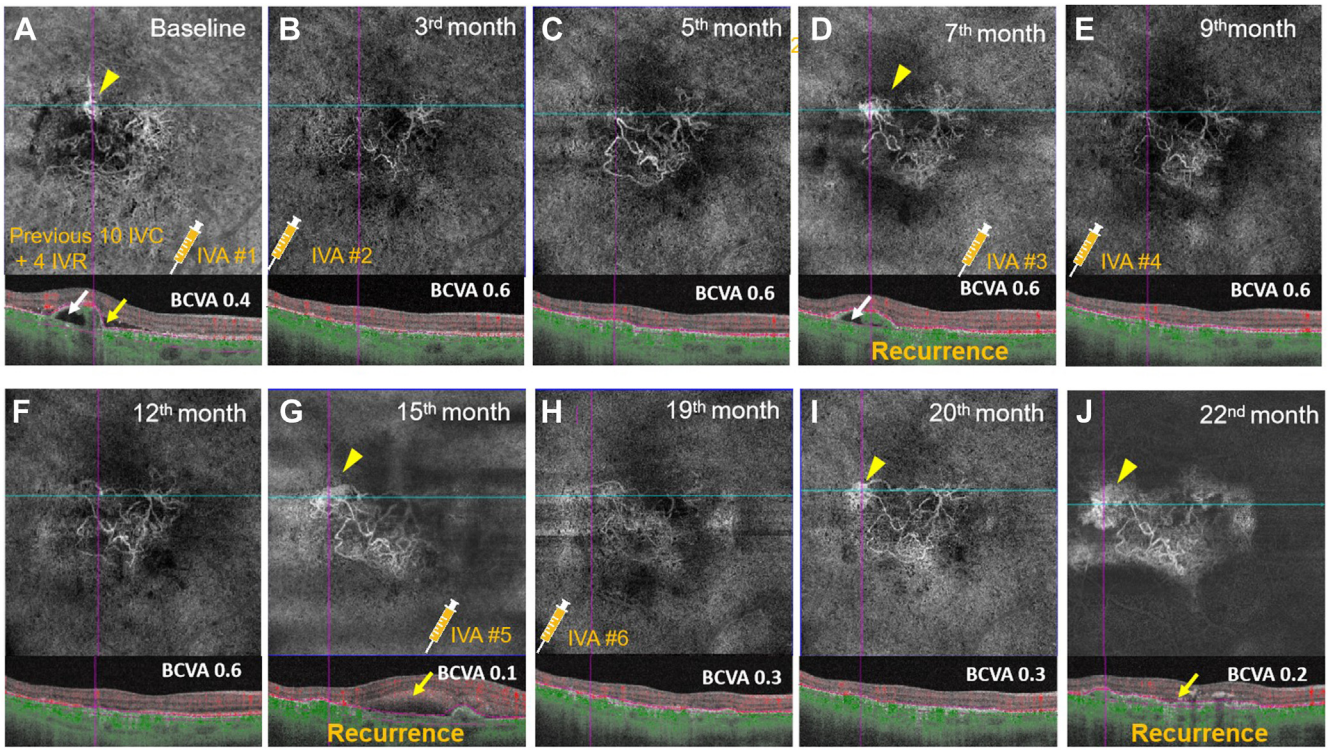

Figure 6. Swept-source OCT angiography (SS-OCTA) images displaying multiple exudative recurrences in a 65-year-old woman after 10 intravitreal injections of conbercept and 4 intravitreal injections of ranibizumab (IVR) before her first SS-OCTA visit. **A,** The 6 × 6-mm en face SS-OCTA and corresponding OCT B-scan images show an exudative polypoidal choroidal vasculopathy (PCV) lesion with 1 polypoidal lesion (yellow arrow). **B,** Regression of polypoidal lesion, branching vascular network (BVN), subretinal fluid (SRF), and serous pigment epithelium detachment (PED) 1 month after 2 intravitreal injections of aflibercept (IVA). **C,** En face SS-OCTA image showing nonexudative growth of BVN 2 months later. **D,** Reappearance of the polypoidal lesion (yellow arrowhead) and PED was identified at the 7-month visit, indicating the first exudative recurrence of the lesion. The third aflibercept injection was administered at this visit. **E, F,** Swept-source OCTA images showing complete regression of polypoidal lesions and partial shrinkage of BVN after the fourth IVA at the 9-month visit. Both polypodal lesions and the BVN remained stable until the 12-month visit. **G.** At the 15-month visit, the second exudative recurrence was detected, as the polypoidal lesion (yellow arrowhead) and exudative features (yellow arrow) reappeared. The fifth aflibercept injection was administered at this visit. **H,** After the sixth aflbercept injection, the polypoidal lesion, BVN, and SRF regressed at the 19-month visit. **I,** Nonexudative BVN growth and polypoidal lesion reappearance detected 1 month later. **J,** Exudative recurrence for the third time occurred 2 months later, with polypoidal lesion enlargement compared with the 20-month visit. BCVA = best-corrected visual acuity; IVC = intravitreal injections of conbercept.

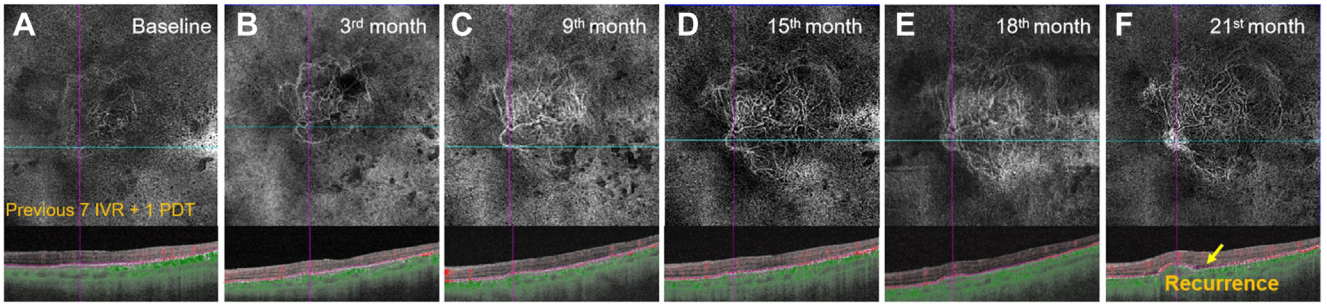

Figure 7. Swept-source OCT angiography (SS-OCTA) images showing a nascent polypoidal lesion developing from the remaining branching vascular network (BVN) in the eye of a 70-year-old woman with polypoidal choroidal vasculopathy (PCV). Baseline en face images and B-scans indicate complete regression of polypoidal lesion with a history of 7 intravitreal injections of ranibizumab (IVR) and 1 session of photodynamic therapy (PDT). **A—E,** The 6 × 6-mm en face SS-OCTA images and corresponding B-scans showing gradual nonexudative growth and extension of the remnant BVN over time. **F,** Swept-source OCTA en face image and OCT B-scan showing the recurrence of exudation and progression of polypoidal lesion at the 21-month visit, with continuous growth of the BVN. BVN aggregation is identified in the en face image, with terminal vessels tangled into a glomerularlike polypoidal lesion, and new onset of subretinal fluid (SRF) (yellow arrow) is presenting in the B-scan image.

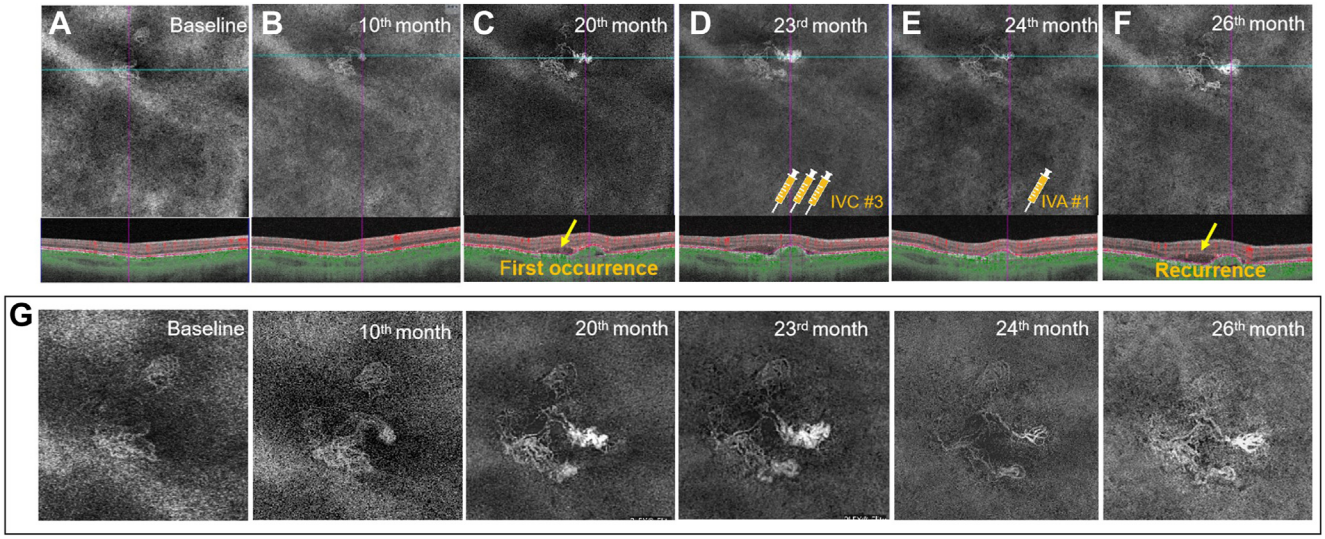

Figure 8. Swept-source OCT angiography (SS-OCTA) (6 × 6 mm) showing the new appearance of polypoidal lesion, first occurrence, and recurrence of exudation in a treatment-naive eye with nonexudative type 1 macular neovascularization (MNV). **A–C,** En face SS-OCTA and B-scan images showing nonexudative growth of MNV and the first occurrence of exudation (yellow arrow). **D, E,** En face SS-OCTA and B-scan images showing exudative remission and lesion shrinkage after 4 anti-VEGF injections (3 intravitreal injections of conbercept and 1 injection of aflibercept [IVA]). **F,** En face SS-OCTA and B-scan images showing the first exudative recurrence with reappearance of the polypoidal lesion 2 months later. **G,** Corresponding 3 × 3-mm en face SS-OCTA images showing gradual growth of the branching vascular network (BVN) over the 26-month follow-up with new appearance, subsequent reduction, and reappearance of the polypoidal lesion. IVC = intravitreal injections of conbercept.

Study Limitations

The limitations of this study include its cross-sectional, retrospective design and the relatively small sample size. Prospective studies using OCTA indicators are warranted to demonstrate the evolution patterns in a larger cohort while evaluating other potential predictors for exudative recurrences, such as age, gender, choroidal vascularity index, and treatment history.[40,41] Most likely, closer follow-up of the nonexudative eyes would have revealed changes that were more closely associated with exudative recurrence than our 3-month interval, which is still not optimal for exploring the predictive correlations between very near-term changes and exudative recurrences. Ideally, we should have included at least 2 near-term nonexudative visits before the exudative recurrence to demonstrate the predictive value of the changes in PCV lesions. However, most patients came back to the clinic only after the exudative recurrence had already occurred, and it was impractical for patients to come in at shorter intervals. Finally, the patients included in this study were treated with both PDT and anti-VEGF therapy, which might result in different outcomes compared with anti-VEGF therapy alone.

Conclusions

Nonexudative BVN growth and polypoidal lesion progression were both characteristics associated with exudative recurrences of PCV. Compared with BVN growth, polypoidal lesion progression was more commonly associated with exudative recurrence. In addition to polypoidal lesions being a significant diagnostic indicator or end point indicator, progression of polypoidal lesions may be a promising and powerful indicator for exudative recurrences. Swept-source OCTA has proven to be a valuable imaging method for detecting the progression of polypoidal lesions and for monitoring eyes with PCV. Closer follow-up could be considered once the progression of these polypoidal lesions is detected. In the future, the predictive role of polypoidal lesion progression needs to be validated, and whether proactive treatment can prevent exudative recurrence of PCV needs to be investigated.

Footnotes and Disclosures

Originally received: February 14, 2022.
Final revision: August 31, 2022.
Accepted: September 12, 2022.
Available online: September 22, 2022. Manuscript no. OPHTHA-D-22-00285.

[1] Department of Ophthalmology, Shanghai General Hospital, Shanghai Jiao Tong University School of Medicine, Shanghai, China.

[2] National Clinical Research Center for Eye Diseases, Shanghai, China.

[3] Shanghai Key Laboratory of Ocular Fundus Diseases, Shanghai, China.

[4] Shanghai Engineering Center for Visual Science and Photomedicine, Shanghai, China.

[5] Shanghai Engineering Center for Precise Diagnosis and Treatment of Eye Diseases, Shanghai, China.

[6] Department of Ophthalmology, Bascom Palmer Eye Institute, University of Miami Miller School of Medicine, Miami, Florida.

*Q.B. and M.Z. contributed equally to this work.

Disclosure(s): All authors have completed and submitted the ICMJE disclosures form. The author(s) have made the following disclosure(s): P.J.R.: Consultant − Annexon, Apellis, Bayer, Boehringer-Ingelheim, Carl Zeiss Meditec, Inc, Chengdu Kanghong Biotech, Ocunexus (inflammX), Ocudyne, Regeneron, Unity Biotechnology; Financial research support −Carl Zeiss Meditec, Inc, Gyroscope Therapeutic, Stealth BioTherapeutics; Equity owner − Apellis, Ocudyne, Valitor, Verana Health.

X.D.S.: Consultant − Novartis, Roche, Alcon, Allergan, Bayer Healthcare, Innovent Biologics Inc, Chengdu Kanghong Biotech, Carl Zeiss Meditec, Inc.

F.H.W.: Consultant −Carl Zeiss Meditec, Inc, Innovent Biologic Inc; Equity owner − Innostellar Biotherapeutics.

Supported by the National Natural Science Foundation of China (81730026, 82171076 and 81970845); National Key R&D Program (2017YFA0105301); Science and Technology Commission of Shanghai Municipality (20Z11900400); Shanghai Hospital Development Center (SHDC2020CR2040B and SHDC2020CR5014); Shanghai Public Health System's Talent Development Plan (GWV-10.2-YQ09); Star Program of Shanghai Jiaotong University (YG2022QN077).

HUMAN SUBJECTS: Human subjects were included in this study. This study was approved by the institutional review board at Shanghai General Hospital and was conducted in accordance with the tenets of the Declaration of Helsinki. Written consent was waived by the institutional review board because of the retrospective nature of the study. All data analyzed were anonymized and de-identified.

No animal subjects were used in this study.

AUTHOR CONTRIBUTIONS

Conception and design: Bo, Wang, X. Sun

Data collection: Bo, Zhang, Chen, M. Sun, Xu, Yu, Feng, Yan, Shen

Analysis and interpretation: Bo, Zhang, Chen, Jia, M. Sun, Xu, Shen, Huang, Li, Wang, Rosenfeld

Obtained funding: Wang, X. Sun, Huang, Bo

Overall responsibility: Bo, Zhang, Li, Wang, Rosenfeld, X. Sun

Abbreviations and Acronyms:
BCVA = best-corrected visual acuity; **BVN** = branching vascular network; **CI** = confidence interval; **ICGA** = indocyanine green angiography imaging; **IRF** = intraretinal fluid; **logMAR** = logarithm of the minimum angle of resolution; **MNV** = macular neovascularization; **OR** = odds ratio; **PCV** = polypoidal choroidal vasculopathy; **PDT** = photodynamic therapy; **PED** = pigment epithelial detachment; **RPE** = retinal pigment epithelium; **SFCT** = subfoveal choroid thickness; **SRF** = subretinal fluid; **SS-OCTA** = swept-source OCT angiography; **VEGF** = vascular endothelial growth factor.

Keywords:
Branching vascular network, Polypoidal choroidal vasculopathy, Polypoidal lesion, Swept-source OCT angiography.

Correspondence:
Xiaodong Sun, MD, PhD, Fenghua Wang, MD, and Tong Li, MD, Department of Ophthalmology, Shanghai General Hospital, Shanghai Jiao Tong University School of Medicine, 100 Haining Road, Shanghai, China, 200080. E-mail: xdsun@sjtu.edu.cn; shretina@sjtu.edu.cn; lindaamadues@163.com.

References

1. Wong CW, Yanagi Y, Lee WK, et al. Age-related macular degeneration and polypoidal choroidal vasculopathy in Asians. *Prog Retin Eye Res*. 2016;53:107−139.
2. Cheung C, Lai T, Teo K, et al. Polypoidal choroidal vasculopathy: consensus nomenclature and non-indocyanine green angiograph diagnostic criteria from the Asia-Pacific Ocular Imaging Society PCV Workgroup. *Ophthalmology*. 2021;128:443−452.
3. Cheung C, Lai T, Ruamviboonsuk P, et al. Polypoidal choroidal vasculopathy: definition, pathogenesis, diagnosis, and management. *Ophthalmology*. 2018;125:708−724.
4. Dansingani KK, Gal-Or O, Sadda SR, et al. Understanding aneurysmal type 1 neovascularization (polypoidal choroidal vasculopathy): a lesson in the taxonomy of 'expanded spectra' - a review. *Clin Exp Ophthalmol*. 2018;46:189−200.
5. Yannuzzi LA, Sorenson J, Spaide RF, Lipson B. Idiopathic polypoidal choroidal vasculopathy (IPCV). *Retina*. 1990;10:1−8.
6. Nowak-Sliwinska P, van den Bergh H, Sickenberg M, Koh AH. Photodynamic therapy for polypoidal choroidal vasculopathy. *Prog Retin Eye Res*. 2013;37:182−199.
7. Oishi A, Kojima H, Mandai M, et al. Comparison of the effect of ranibizumab and verteporfin for polypoidal choroidal vasculopathy: 12-month LAPTOP study results. *Am J Ophthalmol*. 2013;156:644−651.
8. Lim TH, Lai T, Takahashi K, et al. Comparison of ranibizumab with or without verteporfin photodynamic therapy for polypoidal choroidal vasculopathy: the EVEREST II Randomized Clinical Trial. *JAMA Ophthalmol*. 2020;138:935−942.
9. Wong TY, Ogura Y, Lee WK, et al. Efficacy and safety of intravitreal aflibercept for polypoidal choroidal vasculopathy: two-year results of the Aflibercept in Polypoidal Choroidal Vasculopathy Study. *Am J Ophthalmol*. 2019;204:80−89.
10. Miyata M, Ooto S, Yamashiro K, et al. Five-year visual outcomes after anti-VEGF therapy with or without photodynamic therapy for polypoidal choroidal vasculopathy. *Br J Ophthalmol*. 2019;103:617−622.
11. Chen LJ, Cheng CK, Yeung L, et al. Management of polypoidal choroidal vasculopathy: Experts consensus in Taiwan. *J Formos Med Assoc*. 2020;119:569−576.
12. Cheung C, Lai T, Ruamviboonsuk P, et al. Polypoidal choroidal vasculopathy: definition, pathogenesis, diagnosis, and management. *Ophthalmology*. 2018;125:708−724.
13. Waldstein SM, Simader C, Staurenghi G, et al. Morphology and visual acuity in aflibercept and ranibizumab therapy for neovascular age-related macular degeneration in the VIEW Trials. *Ophthalmology*. 2016;123:1521−1529.
14. Kim JH, Chang YS, Kim JW, et al. Submacular hemorrhage and grape-like polyp clusters: factors associated with reactivation of the lesion in polypoidal choroidal vasculopathy. *Eye (Lond)*. 2017;31:1678−1684.
15. Hikichi T. Six-year outcomes of antivascular endothelial growth factor monotherapy for polypoidal choroidal vasculopathy. *Br J Ophthalmol*. 2018;102:97−101.
16. Huang Z, Ding Q, Yan M, et al. Short-term efficacy of conbercept and ranibizumab for polypoidal choroidal vasculopathy. *Retina*. 2019;39:889−895.
17. Tan CS, Ngo WK, Lim LW, et al. Outcomes of polypoidal choroidal vasculopathy treated with ranibizumab monotherapy. *Br J Ophthalmol*. 2013;97:1357−1358.
18. Yang J, Yuan M, Wang E, et al. Five-year real-world outcomes of anti-vascular endothelial growth factor monotherapy

versus combination therapy for polypoidal choroidal vasculopathy in a Chinese population: a retrospective study. *BMC Ophthalmol*. 2019;19:237.
19. Miyata M, Ooto S, Yamashiro K, et al. Five-year visual outcomes after anti-VEGF therapy with or without photodynamic therapy for polypoidal choroidal vasculopathy. *Br J Ophthalmol*. 2019;103:617–622.
20. Kang HM, Koh HJ. Long-term visual outcome and prognostic factors after intravitreal ranibizumab injections for polypoidal choroidal vasculopathy. *Am J Ophthalmol*. 2013;156:652–660.
21. Kang HM, Koh HJ, Lee SC. Baseline polyp size as a potential predictive factor for recurrence of polypoidal choroidal vasculopathy. *Graefes Arch Clin Exp Ophthalmol*. 2016;254:1519–1527.
22. Oishi A, Mandai M, Kimakura M, et al. Characteristics of fine vascular network pattern associated with recurrence of polypoidal choroidal vasculopathy. *Eye (Lond)*. 2011;25:1020–1026.
23. Hikichi T, Higuchi M, Matsushita T, et al. Results of 2 years of treatment with as-needed ranibizumab reinjection for polypoidal choroidal vasculopathy. *Br J Ophthalmol*. 2013;97:617–621.
24. Kwon HJ, Lee JJ, Park SW, et al. Enlargement of polypoidal choroidal vasculopathy lesion without exudative findings assessed in en face optical coherence tomography images. *Graefes Arch Clin Exp Ophthalmol*. 2019;257:1621–1629.
25. Kim JY, Son WY, Kim RY, et al. Recurrence and visual prognostic factors of polypoidal choroidal vasculopathy: 5-year results. *Sci Rep*. 2021;11:21572.
26. Wong CW, Cheung CM, Mathur R, et al. Three-year results of polypoidal choroidal vasculopathy with photodynamic therapy: retrospective study and systematic review. *Retina*. 2015;35:1577–1593.
27. Bo Q, Yan Q, Shen M, et al. Appearance of polypoidal lesions in patients with polypoidal choroidal vasculopathy using swept-source optical coherence tomographic angiography. *JAMA Ophthalmol*. 2019;137:642–650.
28. Chaikitmongkol V, Kong J, Khunsongkiet P, et al. Sensitivity and specificity of potential diagnostic features detected using fundus photography, optical coherence tomography, and fluorescein angiography for polypoidal choroidal vasculopathy. *JAMA Ophthalmol*. 2019;137:661–667.
29. Fujita A, Kataoka K, Takeuchi J, et al. Diagnostic characteristics of polypoidal choroidal vasculopathy based on b-scan swept-source optical coherence tomography angiography and its interrater agreement compared with indocyanine green angiography. *Retina*. 2020;40:2296–2303.
30. Wang Y, Bo Q, Jia H, et al. Small dome-shaped pigment epithelium detachment in polypoidal choroidal vasculopathy: an under-recognized sign of polypoidal lesions on optical coherence tomography? *Eye (Lond)*. 2022;36:733–741.
31. Koh A, Lee WK, Chen LJ, et al. EVEREST study: efficacy and safety of verteporfin photodynamic therapy in combination with ranibizumab or alone versus ranibizumab monotherapy in patients with symptomatic macular polypoidal choroidal vasculopathy. *Retina*. 2012;32:1453–1464.
32. Choi S, Kang HM, Koh HJ. Clinical characteristics of super stable polypoidal choroidal vasculopathy after initial remission with anti-VEGF monotherapy. *Graefes Arch Clin Exp Ophthalmol*. 2021;259:837–846.
33. Cheung CM, Yang E, Lee WK, et al. The natural history of polypoidal choroidal vasculopathy: a multi-center series of untreated Asian patients. *Graefes Arch Clin Exp Ophthalmol*. 2015;253:2075–2085.
34. Uyama M, Wada M, Nagai Y, et al. Polypoidal choroidal vasculopathy: natural history. *Am J Ophthalmol*. 2002;133:639–648.
35. Wakabayashi T, Gomi F, Sawa M, et al. Intravitreal bevacizumab for exudative branching vascular networks in polypoidal choroidal vasculopathy. *Br J Ophthalmol*. 2012;96:394–399.
36. Shen M, Zhang Q, Yang J, et al. Swept-source OCT angiographic characteristics of treatment-naive nonexudative macular neovascularization in AMD prior to exudation. *Invest Ophthalmol Vis Sci*. 2021;62:14.
37. Wakazono T, Yamashiro K, Oishi A, et al. Recurrence of choroidal neovascularization lesion activity after aflibercept treatment for age-related macular degeneration. *Retina*. 2017;37:2062–2068.
38. Shen M, Rosenfeld PJ, Gregori G, Wang RK. Predicting the onset of exudation in treatment-naive eyes with nonexudative age-related macular degeneration. *Ophthalmol Retina*. 2022;6:1–3.
39. Shen M, Bo Q, Song M, et al. Replacement of polyps with type 1 macular neovascularization in polypoidal choroidal vasculopathy imaged with swept source OCT angiography. *Am J Ophthalmol Case Rep*. 2021;22:101057.
40. Kuroda Y, Yamashiro K, Miyake M, et al. Factors associated with recurrence of age-related macular degeneration after antivascular endothelial growth factor treatment: a retrospective cohort study. *Ophthalmology*. 2015;122:2303–2310.
41. Shen M, Zhou H, Kim K, et al. Choroidal changes in eyes with polypoidal choroidal vasculopathy after anti-VEGF therapy imaged with swept-source OCT angiography. *Invest Ophthalmol Vis Sci*. 2021;62:5.

Scan code to view VIDEO

PEELED INTERNAL LIMITING MEMBRANE REPOSITION FOR IDIOPATHIC MACULAR HOLES

A Pilot Randomized Controlled Trial

TIAN TIAN, MD, PhD,* HONGSHENG TAN, PhD,† XIUYU ZHU, MD,* XIANG ZHANG, MD,* PEIQUAN ZHAO, MD, PhD*

Purpose: To compare the functional and anatomical outcomes of peeled internal limiting membrane reposition and traditional internal limiting membrane peeling for the treatment of idiopathic macular hole.

Methods: This is a randomized, single-center, and double-blinded, pilot, controlled trial.

Results: Of the 30 patients enrolled, 27 (13 in Group 1 and 14 in Group 2) were included in the primary analysis (22 women [81.5%]; mean [SD] age, 61.7 [6.8] years). The BCVA was 0.23 ± 0.18 logMAR in the reposition group and 0.44 ± 0.24 logMAR in the peeling group at 6 months postoperatively ($P = 0.02$). The primary MH closure rate is 86.7% in the reposition group and 93.3% in the peeling group ($P = 0.60$). The range of the inner retinal dimpling was significantly lower in the reposition group at 6 months postoperatively ($P < 0.0001$). The thickness of the full parafovea ($P = 0.0092$), inner parafovea ($P = 0.0007$), inner perifovea ($P = 0.0044$), and outer fovea ($P = 0.0392$) was significantly greater in the reposition group than that in the peeling group at 6 months postoperatively. The sensitivity threshold and mfERG P1 wave amplitude density in rings one, four, and five were higher in the reposition group than in the peeling group at 6 months postoperatively.

Conclusion: Our findings suggest that the novel technique of peeled internal limiting membrane reposition has advantages over the traditional internal limiting membrane peeling in better microstructural outcomes of inner retina and functional recoveries. Furthermore, larger RCT studies are warranted.

RETINA 43:191–199, 2023

In full-thickness idiopathic macular hole (IMH) surgery, the peeling of the internal limiting membrane (ILM) during vitrectomy is a common surgical step, which leads to a significant improvement in surgical anatomical results.[1] However, since the presence of a dissociated optic nerve fiber layer was first reported after ILM peeling,[2–4] several studies have reported the effect of ILM peeling on the inner layers of the retina, including a progressive reduction of the thickness of the ganglion cell–inner plexiform layer and reduced recovery of b-wave amplitude on focal electroretinography.[5,6] Investigators even reported the occurrence of progressive macular thinning for at least 2 years after successful macular hole (MH) closure with ILM peeling.[7] More recently, Zofia Michalewska et al confirmed that ILM peeling might also alter blood flow in the deep retinal vessels below the peeling area.[8]

The ILM is the basement membrane of the retinal Müller cells and is composed of collagen fibers, glycosaminoglycans, laminin, and fibronectin.[9] The microstructural changes in ILM-peeling areas of the

From the *Department of Ophthalmology, Xinhua Hospital, Affiliated to Medicine School of Shanghai Jiaotong University, Shanghai, China; and †Clinical Research Institute, Shanghai Jiao Tong University School of Medicine, Shanghai, China.

None of the authors has any financial/conflicting interests to disclose.

Supplemental digital content is available for this article. Direct URL citations appear in the printed text and are provided in the HTML and PDF versions of this article on the journal's Web site (https://www.retinajournal.com/).

Reprint requests: Peiquan Zhao, MD, PhD, Department of Ophthalmology, Xinhua Hospital, Affiliated to Medicine School of Shanghai Jiaotong University, No. 1665, Kongjiang Road, Shanghai 200092, China; e-mail: zhaopeiquan@xinhuamed.com.cn

macula region suggest a loss of longitudinal support of the Müller cells. To achieve better anatomical and further functional recovery, we described a novel technique for reposition of the fixed ILM flap with the assistance of perfluoro-n-octane (PFO). Our previous study demonstrated that the peeled ILM reposition achieved better microstructural outcomes for the inner retina compared with conventional ILM peeling in IMH surgery.[10] Here, we report the findings of this pilot study, discuss the practicality of the protocol, and investigate whether the efficacy and safety of the interventions show a trend warranting a large-scale RCT.

Methods

Study Design

This pilot study is a randomized, single-center, double-blinded controlled trial with a parallel two-arm group conducted at the Xinhua Hospital in Shanghai, China. The study adhered to the tenets of the Declaration of Helsinki and is registered at www.clinicaltrials.gov under the identifier NCT03020459. Institutional review board approval (Xinhua Hospital IRB no. XHEC-C-2016) and patients' written informed consent were obtained before enrollment. The trial protocol can be found in **Supplement 1** (**Supplemental Digital Content 1**, http://links.lww.com/IAE/B836). This study followed the Consolidated Standards of Reporting Trials (CONSORT) reporting guideline.

Participants

Participants were recruited from January 2017 to January 2019 at the Department of Ophthalmology, Xinhua Hospital, affiliated to Medicine School of Shanghai Jiaotong University. The trial follow-up of the last enrolled subject was completed on August 1, 2019. We enrolled patients diagnosed with IMH with a diameter of $\leq$600 μm, aged 50 to 80 years. IMH was defined as a defect of the foveal retina involving its full thickness from the ILM to the outer segment of the photoreceptor layer with no other accompanying ophthalmic disorders. The exclusion criteria were traumatic macular hole, a history of intraocular surgery, presence of staphyloma, combination with epiretinal membrane, diabetic retinopathy, hypertensive retinopathy, and other ocular diseases that could influence macular microstructure or visual function. Patients with high myopia (spherical equivalent ≥ -6.0 diopters or axial length $\geq$ 26 mm) were also excluded. Patients are free to withdraw from participation in this study at any time upon request (reasons for withdrawal will be recorded). The patients may be withdrawn from the study for any reasons. If a patient discontinues from the study, he or she will not be allowed to re-enter the study.

Outcome Measures

At baseline, a detailed demographic and medical history was collected. BCVA measure using a standard Snellen chart, spectral-domain OCT scanning (RTVueXR Avanti; Optovue Inc, Fremont, CA), microperimetry (MAIA, CenterVue, Italy), multifocal electroretinogram (mfERG, Espion, Diagnosys LLC, Cambridge, United Kingdom), M-chart (Inami Co, Tokyo, Japan), and NEI-VFQ-25 questionnaires were performed preoperatively and at each time point postoperatively (1, 3, and 6 months). BCVA was converted to logarithm of the minimum angle of resolution values (logMAR) for statistical analysis. Radial B-scans (12 lines) and 3D wide-field en-face methods was used to scan the macula with OCT preoperatively and postoperatively (1, 3, and 6 months). With the Thickness Map protocol of the OCT, the full retinal thickness (from ILM to retinal pigment epithelium), inner retinal thickness (from ILM to inner plexiform layer (IPL)), and outer retinal thickness (from IPL to retinal pigment epithelium) of the fovea, parafovea, and perifovea were recorded, respectively. The range of inner retinal dimplings was recorded as clocks based on the Radial Lines B-scan. Metamorphopsia score (M-score) measurement was performed using the M-chart according to a previously described method.[11]

Randomization and Masking

Eligible patients were randomly assigned (at a 1:1 ratio) to either the ILM peeling reposition group (group 1, n = 15) or the ILM peeling group (group 2, n = 15). Randomization was ensured using simple random assignment by a random number generator (SAS 9.4 software; SAS Institute Inc, NC). Investigators from the Clinical Research Institute generated the random allocation sequence. The principal investigators (T.T., Z.P.Q.) enrolled participants based on the randomization scheme. The allocation was concealed in opaque envelopes at the beginning of the intervention/control period. The participants, the examiner (Z.X.), and the investigators (T.T., Z.X.Y.) who undertook the visual function evaluation of the participants were masked to the treatment allocation. The investigator from the Clinical Research Institute who was responsible for the statistical analysis was also

masked. A vitreoretinal surgeon (Z.P.Q.), who performed the surgical intervention, remained unmasked.

Study Treatments

All patients received standard 3-port pars plana vitrectomy. Combined phacoemulsification with a posterior chamber intraocular lens implantation was conducted in patients with visually significant cataracts or incipient cataracts. The surgery was performed by a single surgeon (P.Z.) using the Constellation 23-gauge vitrectomy system (AlconLaboratories Inc, Fort Worth, TX). The ILM was stained using 0.1 mL of Brilliant Blue G (Brilliant Peel; Geuder, Germany) for approximately 1 minute after stopping the infusion, after which, excess dye was removed.

Investigational Treatment

After dying, a horizontal ILM strip was peeled from the inferior quadrant of the macular area. Then, the ILM was peeled from the inferior to superior area continuously. The "ILM roll" was unfolded with assistance of perfluoro-n-octane (PFO). Finally, the position of the fixed ILM flap was adjusted under a PFO bubble using a flute needle or forceps. The surgical video of this novel technique is provided as **Supplement 2** (**Supplemental Digital Content 2**, http://links.lww.com/IAE/B837). This was followed by a complete fluid–gas exchange using 14% perfluoropropane gas. Patients were instructed to maintain the facedown position for two weeks postoperatively.

Reference Treatment

After dying, the strand of ILM was peeled off radially from the foveal center to the vascular arcade. As a result, a round-shaped, 2.5-disk diameter to 3.5-disk diameter ILM-peeled area was created. This was followed by a complete fluid–gas exchange using 14% perfluoropropane gas. Patients were instructed to maintain facedown position for 2 weeks postoperatively.

Statistical Analysis

Continuous variables were presented as means ± SDs if the parameter followed a normal distribution or as median [interquartile range] if the distribution was not normally distributed. Statistical analysis was performed using SAS 9.4 software (SAS Institute Inc, NC). The univariate analysis of variance was used for parametric analysis. Changes in the replies to the NEI-VFQ25 were reported using a scale ranging from 0 to 100, as described previously.[12] The Student *t*-test and the Wilcoxon rank–sum test were used for comparison of continuous variables. Categorical variables were analyzed using Fisher exact test as needed. *P* values of < 0.05 were considered significant.

Analysis of the Primary Outcome

The BCVA was converted to logMAR for statistical analysis. Student paired *t* test or Wilcoxon signed rank test was performed for the BCVA change between the two groups and within-group comparisons from baseline to the last follow-up. The BCVA of the treatment and control groups at 6 months postoperatively was tested with Student independent *t*-test or Wilcoxon rank–sum test.

Analysis of the Secondary Outcomes

The MH closure rate was tested with the chi-square test and Fisher exact test as needed. The range of inner retinal dimpling was presented as the median (range) and was tested using the Wilcoxon rank–sum test. Postoperative retinal thickness was tested with Student independent *t*-test or Wilcoxon rank–sum test. The fixation stability and sensitivity threshold measured by microperimetry were tested with Student independent *t*-test or Wilcoxon rank–sum test. Student independent *t*-test or Wilcoxon rank–sum test was also be used to test the mfERG P1 wave density amplitudes, M-score values, and NEI-VFQ-25 questionnaire scores.

Results

Study Participants

Patients were randomly assigned to either the ILM peeling reposition group (Group 1, n =15) or the ILM peeling group (Group 2, n = 15). There were no significant differences in baseline characteristics between the two groups for sex, age, duration, MH diameter, and axial length (Table 1). Two patients in the reposition group and one patient in the peeling group experienced persistent MH after the initial operation. The two patients in reposition group received ILM peeling. One patient in the peeling group received extended ILM peeling. Because the analysis of this study was closely based on the surgical method, we performed per-protocol set analysis. Finally, 13 patients in the reposition group and 14 patients in the peeling group were included in per-protocol set (Figure 1). All participants were included to analyze the MH closure rate.

Primary Outcome

The results of BCVA assessments are shown in Table 2 and eTable 1 (**Supplemental Digital Content 3**,

Table 1. Baseline Characteristics

Parameters	Reposition Group	Peeling Group	*P*
BCVA, logMAR	0.89 ± 0.42	0.90 ± 0.51	0.96*
Sex (F/M), n	11/2	11/3	1.000†
Age	62.1 ± 6.5 y	61.9 ± 6.9 y	0.914†
Duration	4.8 ± 6.1 m	2.8 ± 3.1 m	0.267†
MH diameter	371.1 ± 113.9 mm	365.9 ± 155.7 mm	0.917†
Axial length	24.20 ± 1.41	24.26 ± 1.43	0.917†

*Wilcoxon rank–sum test.
†Student *t* test.
logMAR, logarithm of the minimum angle of resolution; MH, macular hole.

http://links.lww.com/IAE/B830). BCVA significantly improved over the 6 months in both the groups. In the peeling group, the BCVA improved from 0.89 ± 0.42 logMAR to 0.23 ± 0.18 logMAR ($P = 0.0005$) at the 6-month follow-up visit. In the reposition group, the BCVA improved from 0.90 ± 0.51 logMAR to 0.44 ± 0.24 logMAR ($P = 0.0006$). At the 6-month follow-up visit, the BCVA was better in the reposition group than in the peeling group (0.23 ± 0.18 logMAR vs. 0.44 ± 0.24 logMAR; $P = 0.02$). No statistical differences in BCVA were detected between the reposition group and the peeling group at baseline (logMAR 0.89 ± 0.42 vs. logMAR 0.90 ± 0.51; $P = 0.96$), 1 month (logMAR 0.46 ± 0.22 vs. logMAR 0.67 ± 0.33; $P = 0.07$), and 3 months postoperatively (logMAR 0.37 ± 0.18 vs. logMAR 0.51 ± 0.22; $P = 0.07$). The mean change in BCVA between the two groups was not significantly different at each follow-up (Table 2). The BCVA of the participants is shown in eTable 1 (**Supplemental Digital Content 3**, http://links.lww.com/IAE/B830) and the line chart is shown in Figure 2.

Secondary Outcomes

Macular hole closure rate and range of inner retinal dimpling. At the 1-month follow-up visit, MH

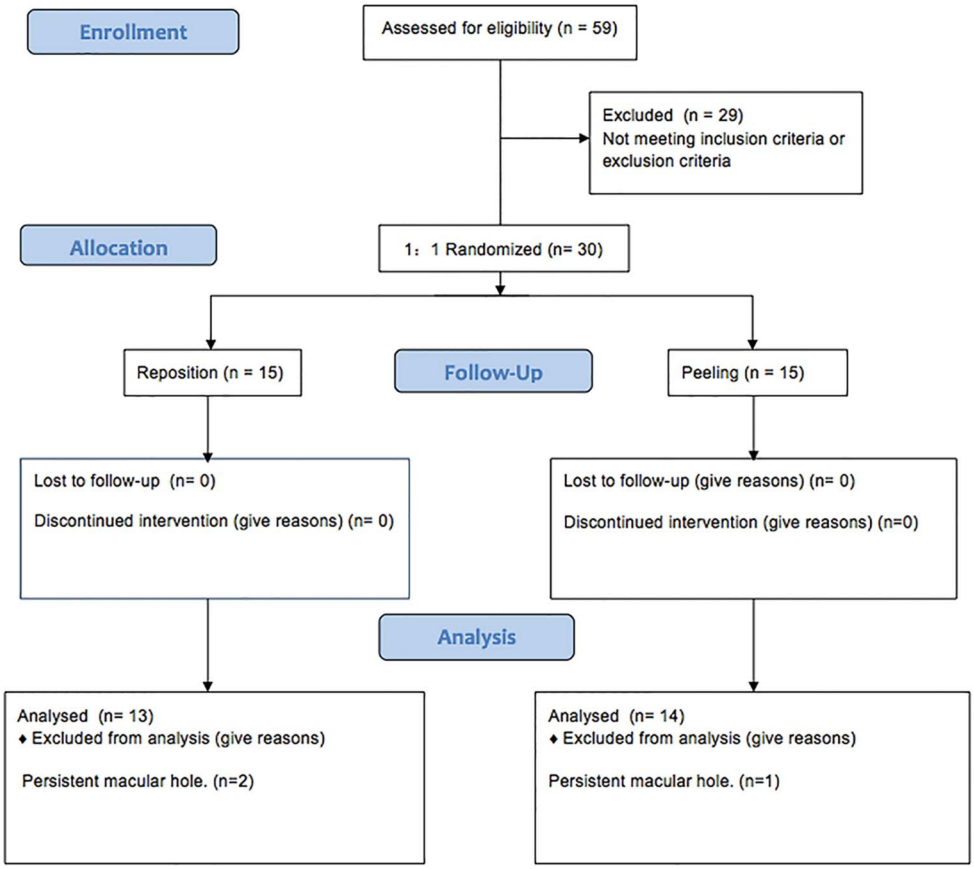

Fig. 1. Study flowchart.

Table 2. Best-Corrected Visual Acuity and Macular Hole Closure Rate

Parameters	Reposition Group	Peeling Group	*P*
BCVA, logMAR			
Preoperation	0.89 ± 0.42*	0.90 ± 0.51†	0.96‡
Postoperative 1m	0.46 ± 0.22	0.67 ± 0.33	0.07§
Postoperative 3m	0.37 ± 0.18	0.51 ± 0.22	0.07§
Postoprative 6m	0.23 ± 0.18[a]	0.44 ± 0.24[b]	0.02§
Postoperative 1m (improvement)	0.43 ± 0.41	0.23 ± 0.44	0.16‡
Postoperative 3m (improvement)	0.52 ± 0.40	0.39 ± 0.42	0.41‡
Postoprative 6 m (improvement)	0.66 ± 0.51	0.46 ± 0.38	0.26§
MH closure rate	86.70%	93.30%	0.60¶

*P = 0.0005 (Student t test).
†P = 0.0006 (Student t test).
‡Wilcoxon rank–sum test.
§Student t test.
¶Fisher exact test.
logMAR, logarithm of the minimum angle of resolution; y, years old; m, months; MH = macular hole.

closure was observed in 13 participants (86.7%) in the reposition group compared with 14 participants (93.3%) in the peeling group (P = 0.60, Table 2). The two patients in reposition group received ILM peeling and one patient in the peeling group received extended ILM peeling. The final closure rate is 100% in two groups. Final analysis of 27 patients demonstrated that the range of the inner retinal dimpling was significantly lower in the reposition group than in the peeling group at 1 month (0, 0–2 clocks vs. 0, 0–12 clocks, P = 0.04), 3 months (0, 0–4 clocks vs. 10.5, 3–12 clocks, $P < 0.0001$), and 6 months (0, 0–10 clocks vs. 11, 7–12 clocks, $P < 0.0001$) postoperatively (median, min–max; **eTable 2** (**Supplemental Digital Content 4**, http://links.lww.com/IAE/B831)). Inner retinal dimpling was observed in only one patient (7.7%) in the reposition group compared with six patients (42.9%) in the peeling group at one month postoperatively. In the reposition group, inner retinal dimpling was observed in three patients (23.1%) at three months and in five patients (38.5%) at 6 months postoperatively. Notably, the dimples were mainly located in the peeled ILM strip area (not ILM covered) in the reposition group. In the peeling group, the dimples developed quickly after one month, and all 14 eyes (100%) had inner retinal dimpling at three and 6 months postoperatively. Comparative analysis of a patient who previously underwent traditional ILM peeling of the left eye and was later enrolled in the study for the peeled ILM repositioning of the right eye is shown in Figure 3. The eye that received ILM reposition showed noticeably less formation of inner retinal dimpling than the eye that received the traditional ILM peeling. In the reposition group, the preserved ILM was in place in all but one patient during the 6-month follow-up. We observed a rolled-up reposition ILM flap at the 3-month follow-up in this patient. Interestingly, inner retinal dimpling was not obvious at the 3-month follow-up, but the dimples developed quickly during 3 months and 6 months postoperatively in this patient (Figure 4).

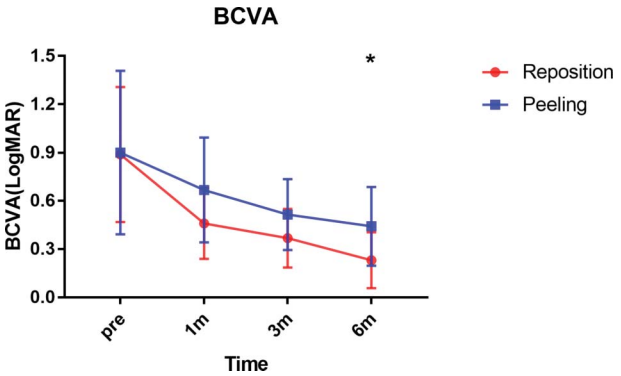

Fig. 2. The line chart of BCVA changes in the two groups. Line chart of best-corrected visual acuity (BCVA) changes of two groups preoperatively and postoperatively. No statistical differences in BCVA were detected between the reposition group and the peeling group at baseline (0.89 ± 0.42 vs. 0.90 ± 0.51; P = 0.96), one month (0.46 ± 0.22 vs. 0.67 ± 0.33; P = 0.07), and three months (0.37 ± 0.18 vs. 0.51 ± 0.22; P = 0.07) postoperatively. At the 6-month follow-up visit, the BCVA was better in the reposition group than in the peeling group (logMAR 0.23 ± 0.18 vs. logMAR 0.44 ± 0.24; P = 0.02). * P value ≤ 0.05.

Retinal Thickness

The full and outer thickness of the fovea, parafovea, and perifovea showed no significant differences between the two groups at 1, 3, and 6 months postoperatively. The mean thickness of the inner fovea was greater in the peeling group than that in the corresponding area in the reposition group at 1 month (78.38 ± 14.23 μm vs. 96.07 ± 26.58 μm; P = 0.04), 3 months (76.33 ± 12.94 μm vs. 91.31 ± 18.03 μm; P = 0.02), and 6 months (80.80 ± 10.45 um vs. 101.00 ± 27.51 μm; P = 0.02) postoperatively. At the 6-month follow-up visit, the thickness of the inner parafovea (126.30 ± 6.36 μm vs. 116.46 ± 11.58 μm; P = 0.01) and inner perifovea (111.70 ± 5.58 μm vs. 102.77 ± 10.35 μm; P = 0.01) was greater in the reposition group than in the peeling

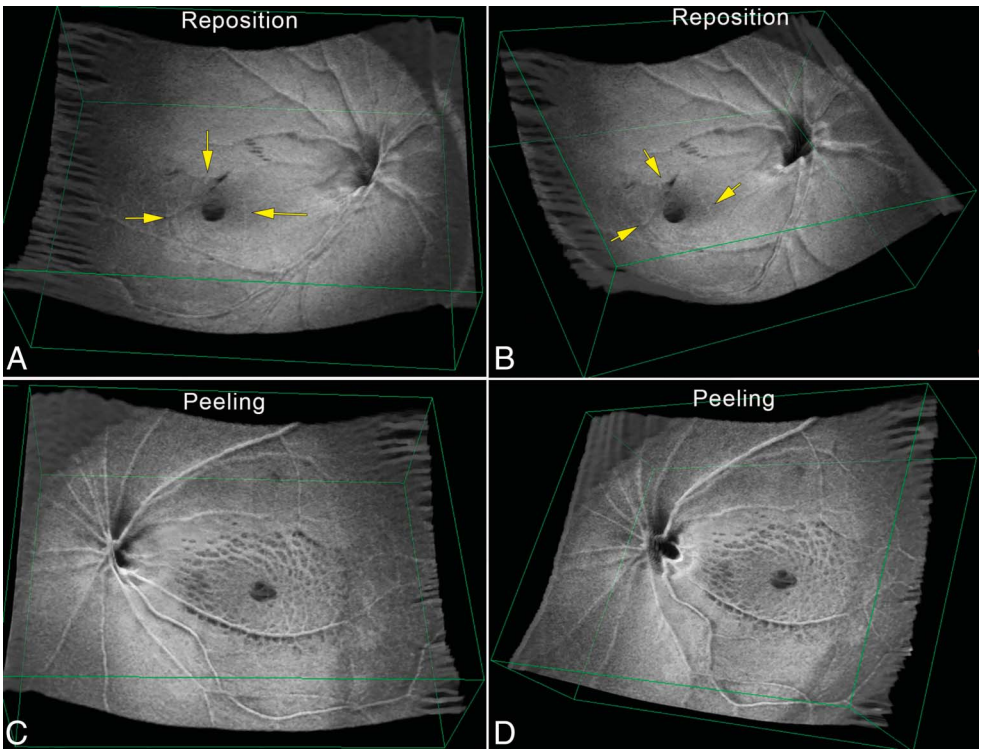

Fig. 3. Postoperative en-face scanning of two eyes in one patient who received two different surgical interventions. Postoperative en-face spectral-domain optical coherence tomography (SD-OCT) of one patient who had previously had traditional ILM peeling in the left eye and was later enrolled in the study for peeled ILM repositioning in the right eye. **A** and **B.** No inner retinal dimpling was detected in the right eye, which received peeled ILM repositioning, at 6 months postoperatively. The margin of the preserved ILM flap can be observed (*yellow arrows*). **C** and **D.** Obvious formation of inner retinal dimpling was observed in the ILM peeled area in the left eye, which received traditional ILM peeling, at 24 months postoperatively.

group. In the ILM peeling group, macular edemas were observed in five patients (35.7%) during follow-up, but no patient experienced macular edema in the reposition group, with no statistical differences ($P = 0.259$). Excluding patients with macular edema, the thicknesses of the full parafovea (322.90 ± 13.63 μm vs. 298.66 ± 29.43 μm; $P = 0.0092$), inner parafovea (126.30 ± 6.36 μm vs. 113.05 ± 9.16 μm; $P = 0.0007$), inner perifovea (111.70 ± 5.58 μm vs. 100.09 ± 11.00 μm; $P = 0.0044$), and outer fovea (194.70 ± 12.96 μm vs. 179.38 ± 19.71 μm; $P = 0.0392$) were significantly greater in the reposition group than in the peeling group at 6 months postoperatively (see **eFigure 1**, **Supplemental Digital Content 5**, http://links.lww.com/IAE/B829).

Microperimetry Assessment

The fixation stability was lower in the reposition group than in the peeling group at baseline (P1: 63.77% ± 16.63% vs. 78.21% ± 19.18%; $P = 0.03$; P2: 89.855 ± 6.11% vs. 95.14% ± 6.13%; $P = 0.01$). However, no statistically significant difference in

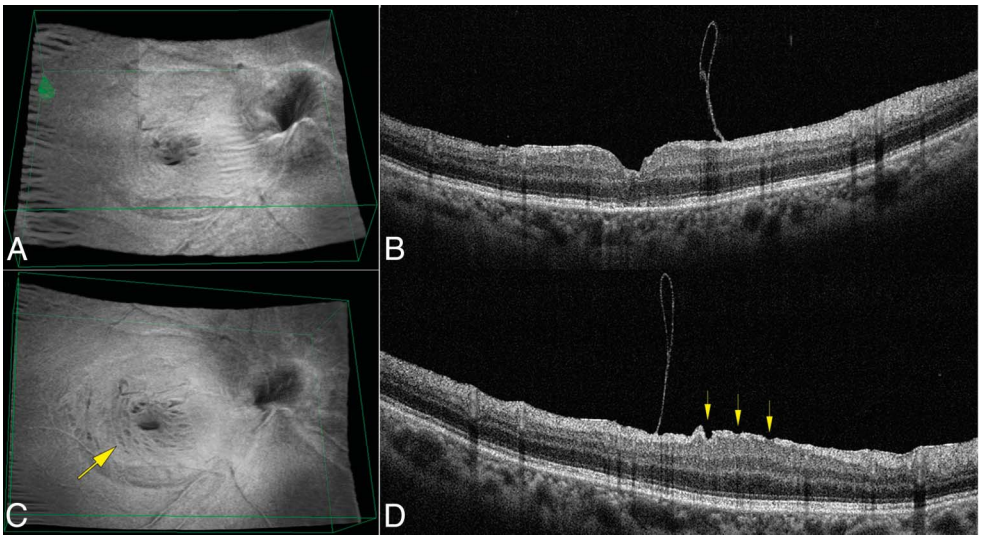

Fig. 4. Postoperative en-face scanning of one patient who received ILM reposition. Postoperative en-face spectral-domain optical coherence tomography (SD-OCT) and B-scan of a patient who underwent pars plana vitrectomy (PPV) with peeled ILM repositioning. **A** and **B.** B-scan showing that the repositioned ILM flap rolled up at the three-month follow-up. No obvious inner retinal dimpling was observed in the en-face scanning. **C** and **D.** At the 6-month follow-up, inner retinal dimpling was detected in the area without ILM coverage (*yellow arrows*).

fixation stability was detected between the two groups at 6 months postoperatively (P1: 83.00% ± 16.84% vs. 80.64% ± 14.78%; $P = 0.61$; P2: 95.69% ± 8.88% vs. 96.57% ± 4.11%; $P = 0.54$). There was no statistical difference in the TS at baseline. The TS was higher in the reposition group than in the peeling group at 3 months (26.52 ± 2.17 dB vs. 24.06 ± 2.54 dB; $P = 0.009$) and 6 months (28.42 ± 1.07 dB vs. 24.91 ± 1.87 dB; $P < 0.0001$) postoperatively, but there was no statistical difference at 1 month postoperatively (24.83 ± 2.29 dB vs. 23.14 ± 3.49 dB; $P = 0.15$) (see **eTable 3**, **Supplemental Digital Content 6**, http://links.lww.com/IAE/B832).

mfERG, M-Score Values, and NEI-VFQ-25 Questionnaire Scores

For the reposition group, the mfERG P1 wave amplitude density were higher in ring four at 1 month postoperatively (5.32 ± 2.10 vs. 6.89 ± 1.48; $P = 0.03$). At the 6-month follow-up, the mfERG P1 wave amplitude density was higher in ring 1 (20.70 ± 6.45 vs. 16.51 ± 5.78; $P = 0.04$), ring 4 (8.92 ± 2.00 vs. 6.84 ± 2.19; $P = 0.02$), and ring 5 (7.95 ± 2.02 vs. 6.08 ± 1.90; $P = 0.02$) in the reposition group than that in the peeling group. For the remaining mfERG P1 wave amplitude density, there was no statistical difference between the two groups (see **eTable 4**, **Supplemental Digital Content 7**, http://links.lww.com/IAE/B833). Metamorphopsia vertical scores (median, 0.5; range, 0.2–0.9 score; vs. median, 0.45; range, 0.2–0.7 score; $P = 0.90$) and horizontal scores (median, 0.5; range, 0.2–0.9 score; vs. median, 0.4; range, 0.2–0.7 score; $P = 0.12$) were not statistically different between the two groups at 6 months postoperatively (see **eTable 5**, **Supplemental Digital Content 8**, http://links.lww.com/IAE/B834). The final analysis showed no statistical difference in NEI-VFQ-25 questionnaire scores between the two groups at 6 months postoperatively (83.4 ± 67.9 vs. 87.0 ± 7.0; $P = 0.22$) (see **eTable 6**, **Supplemental Digital Content 9**, http://links.lww.com/IAE/B835).

Safety

Two patients in the reposition group and one patient in the peeling group experienced persistent MH after the initial operation. The two patients in the reposition group received ILM peeling. The one patient in the peeling group received extended ILM peeling. All of the persistent MHs closed after the second surgery, and none of the patients had a reopening of the MH during the follow-up. No other serious postoperative complications, such as recurrence of MH, endophthalmitis, or rhegmatogenous retinal detachment, were observed in either group.

Discussion

This article reports the results of a pilot study and tests the practicality of the RCT design. The efficacy results obtained in the pilot study can be used for calculating the sample size of a further full-scale RCT. Participant enrolled in this pilot study showed acceptable compliance, with no dropouts during the entire trail. The findings suggest that the design of the study is feasible, and the protocol can be executed. In this study, the novel technique of peeled ILM reposition technique achieves better BCVA at 6 months postoperatively as compared with the conventional ILM peeling technique regarding MH closure rate. The main benefit of the peeled ILM reposition technique arises from the better anatomical and functional recoveries achieved in patients with idiopathic MH.

To peel or not to peel the ILM remains one of the unsolved controversies in ophthalmology. For the novel technique of peeled ILM, reposition can relieve the tractive force around the hole that was necessary to close MH successfully and preserve the integrity of retina simultaneously. Thus, the novel technique has advantage over no ILM peeling in increasing retinal mobility and has advantage over traditional ILM peeling in preserving the integrity of retina. The ILM is the base membrane for Müller cells, which have roles in the homeostasis and maintenance of the inner retinal architecture.[13] Müller cells are the primary structure for the fovea, which binds the receptor cells in the foveola together.[14,15] Without this binding, the retinal receptor cells would be highly susceptible to disruption at the foveola.[16]

Recently, the postoperative morphological changes in patients with IMH after undergoing ILM peeling have warranted attention from scholars. In 2001, Tadayoni et al[2] first described numerous arcuate striae directed along the optic nerve fibers after idiopathic epiretinal membrane removal. In 2012, Spaide[17] confirmed the presence of similar inner retinal defects resembling pits or dimples coursing along the NFL on en-face images, naming it "inner retinal dimpling." However, the retinal dimpling seen after ILM peeling affects visual function has been debated for many years and is still unclear as we do not know what the patients' visual function would have been if they did not demonstrate the presence of retinal dimpling. Terasaki et al[6] reported selective delay of the recovery of the focal macular electroretinogram (FMERG) b-wave 6 months after ILM peeling compared with nonpeeling in idiopathic MH surgery. In 2014, Toshio et al investigated ILM peeling and showed that it resulted in damage to the vitreoretinal interface, which lacked complete restoration three years after the procedure.[18] This pilot study provides an opportunity for ophthalmologists to investigate the relationship between visual acuity and retinal dimpling.

In this pilot study, we found that the IMH patients in the reposition group achieved better VA at 6 months postoperatively with less retinal dimpling formation. In the reposition group, the BCVA was better at 6 months after the surgery and improved more quickly within 1 month than that in the peeling group. Besides, higher mfERG P1 wave amplitude density and retinal sensitivity measured by microperimetry were observed in the reposition group at 6 months postoperatively. Previous clinical studies reported that the incidence rates of inner retinal dimpling were 43%–72%,[2–4,17] whereas the study by Franck et al. indicated an incidence of 86%.[13] In this study, the range of inner retinal dimpling was significantly greater in the peeling group than that in the reposition group. It is interesting to observe that only six patients (42.9%) had inner retinal dimpling in the peeling group at 1 month postoperatively. However, the range of dimples developed quickly after 1 month, and all eyes with ILM peeling had inner retinal dimpling at three and 6 months postoperatively. In the reposition group, the preserved ILM flap was in place in all patients except one during the 6-month follow-up. In the one patient in whom the preserved ILM flap was not in place, the reposition ILM flap rolled up without obvious dimples and clinical symptoms at the three-month follow-up. Interestingly, the range of dimples was approximately 10 clocks at the 6-month follow-up in this patient. This phenomenon indicates that the reposition technique largely prevents the formation of inner retinal dimpling rather than covering it. Ganglion cells carry visual information to the brain through the nerve fiber layer. If the ganglion cells are killed by ILM peeling, one would expect a proportional decrease in the visual field extending to the nerve head. The ILM is the base membrane for Müller cells, which support the photoreceptors and neurons guiding light to the photoreceptors. Based on this, a possible explanation for the reposition group's better functional recovery may be that the preserved ILM prevents nerve fibers being directly exposed to the vitreous cavity, contributing to the recovery of Müller cells. The results of this pilot study showed the trend that the IMH patients in the reposition group achieved better VA at 6 months postoperatively with less retinal dimpling formation. However, the small size of this pilot study limits our certainty on a conclusion. Further full RCT study with larger number of patients and longer follow-up is needed to investigate the relationship between VA and retinal dimpling.

In this study, the thickness of the inner parafoveal and inner perifoveal areas was greater in the reposition group than in the peeling group at the 6-month follow-up. However, the mean thickness of the inner fovea was greater in the peeling group than in the reposition group at one, three, and 6 months postoperatively. To eliminate the effect of macular edema, statistical analysis was performed again after excluding the five patients with macular edema in the peeling group. The results showed that the thickness of the full parafoveal, inner parafoveal, inner perifoveal, and outer foveal areas was greater in the reposition group than in the peeling group at 6 months postoperatively. It has been reported that progressive macular thinning occurs in the extrafoveal macula but not in the fovea after successful MH surgery with ILM peeling and that progressive macular thinning occurs for at least two years postoperatively.[7] The mechanism by which the retina becomes progressively thinner after successful macular surgery with ILM remains unclear. After ILM peeling, the nerve fiber is uncovered and exposed to the vitreous space directly. The ILM is the base membrane for Müller cells that are responsible for the structural stabilization of the retina. In this study, the fixed ILM flap was approximately 1.5-disk diameter to 2.5-disk diameter (2250–3750 μm) wide and 2-disk diameter to 3-disk diameter (3000–4500 μm) long in the reposition group. For the peeling group, the peeled area was approximately 2.5-disk diameter to 3.5-disk diameter (3750–5250 μm). Thus, the parafoveal (1000 μm from the fovea) and perifoveal (2250 μm from the fovea) areas were covered with the preserved ILM flap in the reposition group but not in the peeling group. This finding suggests that the preserved ILM reposition is beneficial for the structural stabilization of the retina and prevents the progressive thinning of the retina compared with total ILM peeling in patients with IMH.

One limitation of the peeled ILM reposition technique is that the use of PFO adds complexity and cost to the surgery. However, the use of PFO is necessary to arrange the position of the preserved ILM flap and can be easily and thoroughly removed by fluid–air exchange. In addition, the peeled ILM reposition technique is not suitable for MH with epiretinal membrane. Even so, the peeled ILM reposition technique preserves the integrity of the retina and can achieve improved BCVA and anatomical recovery compared with conventional ILM peeling at 6 months postoperatively. Indeed, the MH closure rate was lower in the reposition group (86.7%) compared with the peeling group (93.3%) with no statistical difference. Not maintaining the facedown position after surgery was the main cause of unclosed MH in two patients in the reposition group and in one patient in the peeling group. Our study was limited by its single-center design and the small study size. However, the consistency is established with the use of a single surgeon, a team of optometrists, and instrument, all of which reduce bias. Moreover, the BCVA was measured using a standard Snellen chart, which is not more accurate than the early treatment diabetic retinopathy study (ETDRS) method. Because this study is an investigator-initiated clinical trial, considering the difficulty of clinical

implementation, maximum protection of the rights and interests of the subjects, and meeting the needs of hospital ethics and normal working procedures, a more convenient visual acuity assessment method was adopted.

Conclusion

In conclusion, the main finding of this study was that the novel technique of peeled ILM reposition achieves better BCVA as compared with the traditional ILM peeling in treating IMH with a diameter of <600 μm. In addition, the peeled ILM reposition has advantages over the traditional ILM peeling in better microstructural outcomes of inner retina and functional recoveries. Further full-scale RCT study with longer follow-up is needed to determine whether the advantage of the peeled ILM reposition technique will be sustained in the long term.

Study conception and design: T. Tian and P. Zhao. Data collection: T. Tian, X. Zhu, X. Zhang Statistical analysis: X. Zhang and H. Tan Drafting: T. Tian, H. Tan Critical discussion and manuscript revision: T. Tian, P. Zhao and H. Tan. All the authors approved the final version of the manuscript. The data sets used and/or analyzed during the current study are available from the corresponding author on reasonable request.

Key words: idiopathic macular hole, internal limiting membrane, dimplings, surgery, vitrectomy.

Acknowledgments

The authors gratefully acknowledge all the patients who have accepted to take part in this study. This research was supported by the National Natural Science Foundation of China (grant 82000904; grant 82171069, grant 81770964). The funders had no role in the design and conduct of the study; collection, management, analysis, and interpretation of the data; preparation, review, or approval of the manuscript; and decision to submit the manuscript for publication. The manuscript was copyedited for English language by LetPub, with regard to grammar, punctuation, spelling, and clarity.

References

1. Michels RG, Kampik A, Green WR, Nase PK. Ultrastructural features of progressive idiopathic epiretinal membrane removed by vitreous surgery. Am J Ophthalmol 1980;90:797–809.
2. Tadayoni R, Paques M, Massin P, et al. Dissociated optic nerve fiber layer appearance of the fundus after idiopathic epiretinal membrane removal. Ophthalmology 2001;108:2279–2283.
3. Ito Y, Terasaki H, Takahashi A, et al. Dissociated optic nerve fiber layer appearance after internal limiting membrane peeling for idiopathic macular holes. Ophthalmology 2005;112:1415–1420.
4. Mitamura Y, Ohtsuka K. Relationship of dissociated optic nerve fiber layer appearance to internal limiting membrane peeling. Ophthalmology 2005;112:1766–1770.
5. Balducci N, Morara M, Veronese C, et al. Retinal nerve fiber layer thickness modification after internal limiting membrane peeling. Retina 2014;34:655–663.
6. Terasaki H, Miyake Y, Nomura R, et al. Focal macular ERGs in eyes after removal of macular ILM during macular hole surgery. Invest Ophthalmol Vis Sci 2001;42:229–234.
7. Kumagai K, Hangai M, Larson E, Ogino N. Progressive changes of regional macular thickness after macular hole surgery with internal limiting membrane peeling. Invest Ophthalmol Vis Sci 2013;54:4491–4497.
8. Michalewska Z, Nawrocki J. Swept-source optical coherence tomography angiography reveals internal limiting membrane peeling alters deep retinal vasculature. Retina 2018;38:S154–S160.
9. Wollensak G, Spoerl E, Grosse G, Wirbelauer C. Biomechanical significance of the human internal limiting lamina. Retina 2006;26:965–968.
10. Tian T, Chen C, Peng J, et al. Novel surgical technique of peeled internal limiting membrane reposition for idiopathic macular holes. Retina 2019;39:218–222.
11. Arimura E, Matsumoto C, Okuyama S, et al. Quantification of metamorphopsia in a macular hole patient using M-CHARTS. Acta Ophthalmologica Scand 2006;85:55–59.
12. Mangione CM, Lee PP, Gutierrez PR, et al. Development of the 25-list-item national eye Institute visual function questionnaire. Arch Ophthalmol 2001;119:1050–1058.
13. Amouyal F, Shah SU, Pan CK, et al. Morphologic features and evolution of inner retinal dimples on optical coherence tomography after internal limiting membrane peeling. Retina 2014;34:2096–2102.
14. Gass JDM. Muller cell cone, an overlooked part of the anatomy of the fovea centralis: hypotheses concerning its role in the pathogenesis of macular hole and foveomacualr retinoschisis. Arch Ophthalmol 1999;117:821–823.
15. Yamada E. Some structural features of the fovea centralis in the human retina. Arch Ophthalmol 1969;82:151–159.
16. Ohta K, Sato A, Fukui E. Retinal thickness in eyes with idiopathic macular hole after vitrectomy with internal limiting membrane peeling. Graefe's Archive Clin Exp Ophthalmol 2013;251:1273–1279.
17. Spaide RF. Dissociated optic nerve fiber layer appearance" after internal limiting membrane removal is inner retinal dimpling. Retina 2012;32:1719–1726.
18. Hisatomi T, Notomi S, Tachibana T, et al. Ultrastructural changes of the vitreoretinal interface during long-term follow-up after removal of the internal limiting membrane. Am J Ophthalmol 2014;158:550–556.e1.